Articles in PresS. Am J Physiol Renal Physiol (September 22, 2010). doi:10.1152/ajprenal.00011.2010

Rho-associated kinase plays a role in rabbit urethral smooth muscle contraction, but not via enhanced myosin light chain phosphorylation

Michael P. WALSH[1], Keith THORNBURY[2], William C. COLE[3], Gerard SERGEANT[2], Mark HOLLYWOOD[2] and Noel McHALE[2]

[1]*Smooth Muscle Research Group and Department of Biochemistry and Molecular Biology, Faculty of Medicine, University of Calgary, Calgary, Alberta T2N 4N1, Canada,* [2]*Smooth Muscle Research Centre, Dundalk Institute of Technology, Dundalk, Co. Louth, Ireland, and* [3]*Smooth Muscle Research Group and Department of Physiology and Pharmacology, Faculty of Medicine, University of Calgary, Calgary, Alberta T2N 4N1, Canada*

Address for reprint requests and other correspondence: M. P. Walsh, Department of Biochemistry and Molecular Biology, Faculty of Medicine, University of Calgary, Calgary, Alberta T2N 4N1, Canada (email walsh@ucalgary.ca).

Running title: Smooth muscle contraction without an increase in myosin phosphorylation

ABSTRACT

The involvement of Rho-associated kinase (ROK) in activation of rabbit urethral smooth muscle contraction was investigated by examining the effects of two structurally distinct inhibitors of ROK, Y27632 and H1152, on the contractile response to electric field stimulation (EFS), membrane depolarization with KCl, and α_1-adrenoceptor stimulation with phenylephrine. Both compounds inhibited contractions elicited by all three stimuli. The protein kinase C inhibitor, GF109203X, on the other hand, had no effect. Urethral smooth muscle strips were analysed for phosphorylation of three potential direct or indirect substrates of ROK: (i) myosin regulatory light chains (LC_{20}) at S19; (ii) the myosin targeting subunit of myosin light chain phosphatase, MYPT1, at T697 and T855; and (iii) cofilin at S3. The following results were obtained: (i) under resting tension, LC_{20} was phosphorylated to 0.65 $\pm$ 0.02 mol P_i/mol LC_{20} (n = 21) at S19; (ii) LC_{20} phosphorylation did not change in response to KCl or phenylephrine; (iii) ROK inhibition had no effect on LC_{20} phosphorylation in the absence or presence of contractile stimuli; (iv) under resting conditions, MYPT1 was partially phosphorylated at T697 and

T855 and cofilin at S3; (v) phosphorylation of MYPT1 and cofilin was unaffected by KCl or phenylephrine; and (vi) KCl- and phenylephrine-induced contraction-relaxation cycles did not correlate with actin polymerization-depolymerization. We conclude that ROK plays an important role in urethral smooth muscle contraction, but not via inhibition of MLCP or polymerization of actin.

Key words: urethra, urinary continence, myosin light chain phosphatase, cofilin

INTRODUCTION

Lower urinary tract function is dependent on the concerted action of the smooth and striated muscles of the urinary bladder, urethra and periurethral region. Failure to store urine can lead to various forms of incontinence, which is a major health concern (26), but current therapies for incontinence have severe limitations (19). Further therapeutic development will depend on the identification of novel targets. The bladder and urethra work as a functional unit with a reciprocal relationship under normal conditions, i.e., during the storage phase, the detrusor muscle of the bladder is relaxed while the urethra is contracted to allow gradual filling of the bladder with urine and prevent leakage. On the other hand, during voiding, the urethra relaxes and the detrusor contracts to facilitate emptying of the bladder (36). An isolated rat urethral preparation is “continent” in the absence of external neural input, but flow ensues when the smooth muscle is relaxed (29). Furthermore, stimulation of the skeletal muscle makes remarkably little difference to the ability of the contracted urethra to retain fluid. Conte et al (12) also found that paralyzing the striated muscle encircling the urethra of anesthetized rats with d-tubocurarine did not result in urine leakage. It would appear, therefore, that skeletal muscle is more important for resisting rapid pressure rises caused by coughing or laughing, for example, than for maintaining a constant urethral tone, which makes sense from an energetic standpoint. The smooth muscle cells of the urethra, therefore, play a critical role in continence by remaining in a contracted state most of the time, thereby retaining urine within the bladder. This smooth muscle tone can be modified by adrenergic and

cholinergic nerve stimulation (4). Noradrenaline, released by adrenergic neurons, is the major excitatory transmitter in the rabbit urethra (3,13). At the appropriate time, the smooth muscle cells relax in response to inhibitory nerves, and detrusor smooth muscle contraction voids the bladder through a relaxed urethra. Nitric oxide, released by non-adrenergic, non-cholinergic neurons, is an important mediator of urethral smooth muscle relaxation (5,11).

Deficiencies in urethral closure can result in stress urinary incontinence. Treatment of this condition, which is based mainly on α_1-adrenoceptor agonists, has been disappointing (6). In order to improve strategies for treatment of incontinence, it is essential to understand urethral function and regulation in greater detail.

Smooth muscle contraction and relaxation are regulated primarily by the phosphorylation and dephosphorylation of the 20-kDa regulatory light chains of myosin (LC_{20}) (2). Smooth muscle myosin II is a hexameric protein composed of two heavy chains (205 kDa) and two pairs of light chains (17 and 20 kDa). Contraction is activated by an increase in cytosolic free Ca^{2+} concentration ($[Ca^{2+}]_i$), whereupon Ca^{2+} binds to calmodulin (CaM) and the $(Ca^{2+})_4$-CaM complex activates myosin light chain kinase (MLCK). Activated MLCK phosphorylates LC_{20} at S19, resulting in cross-bridge cycling of myosin along the actin filaments and contraction. Relaxation occurs when $[Ca^{2+}]_i$ returns to resting levels upon removal of the contractile stimulus, whereupon LC_{20} is dephosphorylated by myosin light chain phosphatase (MLCP) and myosin dissociates from actin (18).

An important aspect of the regulation of smooth muscle contraction that has emerged in recent years concerns the phenomenon of Ca^{2+} sensitization, i.e., the ability of a variety of agonists to elicit a contractile response without an increase in $[Ca^{2+}]_i$ (33). Ca^{2+} sensitization involves agonist-induced activation of signaling pathways, primarily the RhoA/Rho-associated kinase (ROK) pathway, that terminate in the inhibition of MLCP. This shifts the balance between kinase and phosphatase in favor of

MLCK so that a higher level of LC_{20} phosphorylation (and force) is achieved at a given $[Ca^{2+}]_i$. ROK mediates MLCP inhibition via phosphorylation of the myosin targeting subunit of the phosphatase (MYPT1) at T697 and/or T855 (rat numbering; NCBI accession number EDM16761) (16,31,39) or of the 17 kDa cytosolic protein, CPI-17, which becomes a potent inhibitor of MLCP when phosphorylated at T38 (27).

Studies regarding the role of LC_{20} phosphorylation in urethral contractile physiology have been rather limited. Hypolite et al (21) reported that the rabbit urethra exhibits a low level of basal LC_{20} phosphorylation (12.8%). Modest increases in LC_{20} phosphorylation, from 16% at rest to 28 % at half-maximal bethanecol-induced force, 29% at 80% maximal force and 27% at maximal force, were measured (21). A role for RhoA and ROK in urethral tone was indicated by the demonstration that inhibition of RhoA with *Clostridium difficile* toxin B or of ROK with Y27632 abolished porcine urethral tone without affecting cytosolic free Ca^{2+} concentration (28). ROK inhibition also inhibited the contractile response of rat urethral smooth muscle to phenylephrine, endothelin-1, α,β-methylene ATP and membrane depolarization, but had no significant effect on baseline tension (37).

The overall aim of this work, therefore, was to gain further insights into the molecular mechanisms involved in the regulation of urethral smooth muscle contraction. The following specific questions were addressed: (i) Is the contraction of urethral smooth muscle in response to electric field stimulation, membrane depolarization by KCl or α_1-adrenoceptor stimulation with phenylephrine attenuated by inhibition of ROK? (ii) Does the sustained contraction of urethral smooth muscle involve phosphorylation of LC_{20}? (iii) Does contraction of urethral smooth muscle correlate with the phosphorylation of MYPT1 at T697 and/or T855? (iv) Does the contraction-relaxation cycle of urethral smooth muscle correlate with actin polymerization-depolymerization?

MATERIALS AND METHODS

Materials. Antibodies: rabbit polyclonal anti-calponin was raised in-house against purified full-length chicken gizzard calponin (42). Commercial antibodies were purchased from the following sources: rabbit polyclonal anti-LC_{20} (Santa Cruz Biotechnology) raised against the full-length human protein; rabbit polyclonal anti-pS19-LC_{20} (Rockland) raised against a synthetic phosphopeptide corresponding to the region of the human protein containing pS19; rabbit polyclonal anti-CPI-17 (Upstate) raised against full-length recombinant porcine CPI-17; rabbit polyclonal anti-actin (Cytoskeleton) raised against a synthetic peptide corresponding to the *C*-terminal 11 residues of human actin (SGPSIVHRKCF); goat polyclonal anti-SM-22α (Novus Biologicals) raised against a synthetic peptide (MTGYGRPRQIIS) corresponding to residues 189 - 200 of human SM-22α; rabbit polyclonal anti-pT697-MYPT1 (Upstate) raised against a synthetic phosphopeptide corresponding to the region around pT697 of the human protein; rabbit polyclonal anti-pT855-MYPT1 (Upstate) raised against a synthetic phosphopeptide corresponding to the region around pT855 of the human protein; rabbit polyclonal anti-pS3-cofilin (Cell Signaling Technology) raised against a synthetic phosphopeptide corresponding to human cofilin containing phosphoserine at position 3; rabbit polyclonal anti-cofilin (Cell Signaling Technology) raised against a synthetic peptide corresponding to human cofilin containing serine at position 3. N_{ω}-nitro-L-arginine, atropine, phenylephrine and phorbol 12,13-dibutyrate were purchased from Sigma, Y27632 from BioMol International, H1152, GF109203X, wortmannin and calyculin-A from Calbiochem, and microcystin-LR from Alexis Biochemicals. Molecular weight markers were purchased from Fermenta.

Isolation of urethral tissue for tension measurements. Male New Zealand white rabbits (3 - 4 kg) were maintained and killed with a lethal injection of pentobarbitone according to the standards of the Canadian Council on Animal Care and a protocol approved by the Animal Care Committee of the Faculty of Medicine, University of Calgary, and in accordance with the European Union legislation and

ethical standards. Male Sprague-Dawley rats (250 - 275 g) were maintained and killed by halothane inhalation and decapitation according to the standards of the Canadian Council on Animal Care and a protocol approved by the Animal Care Committee of the Faculty of Medicine, University of Calgary. The proximal 1 cm of the urethra was removed and placed in Krebs solution (120 mM NaCl, 5.9 mM KCl, 25 mM $NaHCO_3$, 5.5 mM glucose, 1.2 mM NaH_2PO_4, 1.2 mM $MgCl_2$, 2.5 mM $CaCl_2$) plus 100 μM N_ω-nitro-L-arginine and 1 μM atropine with pH adjusted to 7.4 with 95% O_2/5% CO_2. The muscarinic antagonist atropine was included to block the effects of acetylcholine released from nerves, and N_ω-nitro-L-arginine to block nitric oxide effects. In separate experiments, we found that omission of these inhibitors had no statistically significant effect on LC_{20} phosphorylation levels, as determined by paired Student's t test: 0.62 ± 0.11 mol P_i/mol LC_{20} in their presence and 0.52 ± 0.10 mol P_i/mol LC_{20} in their absence ($p > 0.05$, $n = 3$). Circularly-oriented strips (8 x 1 x 1 mm) of smooth muscle were dissected. For investigation of the effects of protein kinase inhibitors, muscle strips were placed in a water-jacketed organ bath maintained at 37 ^oC, and perfused with warmed Krebs solution bubbled with 95% O_2/5% CO_2. Strips were adjusted to a tension of 0.5 g, the optimal tension for KCl-induced force development, and allowed to equilibrate for 60 min before experimentation began. During the period of equilibration of the tissue after mounting, it was necessary to stretch the tissue periodically to maintain resting tension at 0.5 g. Stable tension was always achieved within the 60-min equilibration period. Prior experiments indicated that a resting tension of 0.5 g for tissue strips of the dimensions used in this study gave a maximal contractile response to KCl. Contractions in response to electric field stimulation (EFS), KCl and phenylephrine were measured using Statham UC3 and Dynamometer UF1 transducers, with the outputs recorded on a Grass 7400 chart recorder. Tissues did not exhibit significant loss of maximal tension in response to repetitive stimuli (EFS, KCl or phenylephrine) over several hours. Field stimulation was applied via platinum ring electrodes mounted at either end of the tissue strip. Pulses of

0.3 ms duration were delivered in trains at constant frequencies of 4 Hz from a Grass S48 stimulator at a nominal voltage of 50 V. Responses were blocked with 1 μM tetrodotoxin, confirming that they were nerve mediated (38).

Demembranation (skinning) of urethral smooth muscle strips. Urethral smooth muscle strips mounted on a force transducer at resting tension were incubated at 21 ^{o}C with 1% (v/v) Triton X-100 in 30 mM TES, 50 mM KCl, 5 mM K_2EGTA, 150 mM sucrose, 0.5 mM dithioerythritol, pH 7.4 for 2 h. In establishing the optimal conditions for Triton skinning of rabbit urethral smooth muscle strips, the Triton X-100 concentration and time of treatment were varied. The contractile response of the Triton-skinned tissue to Ca^{2+} was comparable to that of the KCl-induced contraction of the intact tissue prior to Triton treatment when 1 % Triton X-100 was used for 2 h. Skinned tissues were then equilibrated with 3.2 mM MgATP, 2 mM free $MgCl_2$, 0.5 mM NaN_3, 30 mM TES, 12 mM phosphocreatine, 15 units/ml creatine kinase, 1 μM calmodulin, pH 6.9 with ionic strength adjusted to 150 mM with potassium propionate. Desired free Ca^{2+} levels were obtained by mixing stock solutions containing K_2EGTA and K_2CaEGTA (41).

Protein extraction. For investigation of protein phosphorylation, muscle strips were immersed in 10% trichloroacetic acid (TCA)/10 mM dithiothreitol (DTT) in acetone that had been pre-cooled on dry ice or wet ice, washed (3 x 1 min) with DTT/acetone, lyophilized overnight and the dried tissues cut into small pieces. SDS-PAGE sample buffer containing 0.1 M DTT (1 ml) was added. Tissue strips of comparable dimensions were extracted with identical volumes of SDS-gel sample buffer, and identical volumes of extract were loaded on gels for western blot analysis. The amount of extract loaded depended on the sensitivity of the individual antibodies utilized. The samples were heated at 95 ^{o}C for 10 min, rotated overnight in the cold room and stored at -20 ^{o}C until SDS-PAGE was performed.

SDS-PAGE. SDS-PAGE was carried out in 1.5-mm thick mini-gels (12.5% acrylamide in the

running gel (15% for CPI-17 analysis) with a 5% acrylamide stacking gel) at 200 V for 45 min in a Mini Protean 3 Cell (Bio-Rad). Following electrophoresis, gels were either stained with Coomassie Brilliant Blue or equilibrated at room temperature for 1 h with Transblot Buffer (25 mM Tris-HCl, pH 7.5, 192 mM glycine, 20% methanol, 0.1% SDS for MYPT1; 10 mM CAPS, pH 11, 10% methanol for CPI-17; 25 mM Tris-HCl, pH 7.5, 192 mM glycine, 20% methanol for the rest) prior to western blotting.

Western blotting. Proteins separated by SDS-PAGE were transblotted to nitrocellulose (0.2 μm; Bio-Rad) at 100 V for 1 h at 4 ^{o}C in a Mini Trans-Blot Electrophoretic Transfer Cell (Bio-Rad). After blotting, the nitrocellulose membrane was washed (3 x 5 min) in PBS (0.137 M NaCl, 2.68 mM KCl, 10 mM Na_2HPO_4, 1.76 mM KH_2PO_4), incubated in 0.5% glutaraldehyde in PBS for 15 min to fix proteins on the membrane and washed (3 x 5 min) with Tris-buffered saline containing Tween 20 (TBST: 20 mM Tris-HCl, pH 7.5, 137 mM NaCl, 3 mM KCl, 0.05% Tween-20). The membrane was then blocked with 5% non-fat dried milk in TBST for 1 h, and incubated overnight at 4 ^{o}C with 1% non-fat dried milk in TBST containing the appropriate primary antibody. Membranes were washed (4 x 5 min) in TBST, incubated with anti-rabbit IgG-horseradish peroxidase-conjugated secondary antibody (1:10,000 dilution in 1% dry milk in TBST; Chemicon) for 1 - 2 h and washed (4 x 5 min) with TBST and (1 x 5 min) with TBS before chemiluminescence signal detection using the Super-Signal West Femto reagent (Pierce). The emitted light was detected and quantified with a chemiluminescence imaging analyzer (LAS3000mini; Fujifilm) and images were analysed with MultiGauge v3.0 software (Fujifilm).

Phosphate affinity SDS-PAGE using acrylamide-pendant phosphate-binding tag. Unphosphorylated and phosphorylated forms of LC_{20} were separated by Phos-tag SDS-PAGE (23,35). Muscle protein samples stored in SDS-PAGE sample buffer at -20 ^{o}C were electrophoresed at 30 mA/gel for 60 min in mini-gels in which 0.05 mM Phos-tag acrylamide (NARD Institute, Japan) and 0.1 mM $MnCl_2$ were incorporated into the running gel. In control experiments, 1 mM EDTA replaced 0.1 mM $MnCl_2$. After

electrophoresis, gels were soaked in Transblot Buffer (25 mM Tris-HCl, pH 7.5, 192 glycine, 10% methanol) containing 2 mM EDTA for 15 min prior to equilibration in Transblot Buffer for 15 min. Proteins were transferred to PVDF (Roche) at 27 V overnight at 4 ^{o}C and fixed with 0.5% glutaraldehyde prior to blocking, etc. as for the normal western blotting procedure described above.

Actin polymerization assay. Actin polymerization was measured using the G-actin/F-actin *in vivo* Assay Kit (Cytoskeleton). Rabbit urethral smooth muscle strips, mounted on a force transducer and equilibrated with Krebs solution at 21 ^{o}C, were treated as described in the appropriate figure legends, homogenized in F-actin stabilization buffer (1 ml) with a Tissue Tearor Model 985-370 Type 2 (Biospec Products) at 21 ^{o}C and centrifuged in a bench-top centrifuge at 2,000 rpm for 5 min. Supernatants were centrifuged at 100,000 x g for 1 h at 21 ^{o}C. The high-speed supernatant was carefully removed and 50 µl of 5X SDS-gel sample buffer added. The high-speed pellet was re-suspended in 250 µl of 1x SDS-gel sample buffer. Samples were heated at 95 ^{o}C for 5 min and stored at -20 ^{o}C prior to SDS-PAGE and western blotting.

Statistical analysis. Statistical analyses were performed with SigmaPlot and Prism. Results are expressed as the means ± S.E.M. Values of *n* indicate the numbers of animals used; several tissue strips were used from each animal. Statistically significant differences were identified by Student's *t* test or one-way ANOVA with Dunnett's post-hoc test as indicated.

RESULTS

Effects of ROK inhibition on urethral smooth muscle contraction. The effects of ROK inhibition on the contractile response of rabbit urethral smooth muscle to EFS, membrane depolarization with KCl, and α_1-adrenoceptor stimulation by phenylephrine were investigated at 37 ^{o}C. Following dissection, mounting and equilibration of the tissue, several control contraction-relaxation cycles were recorded.

The tissue was then incubated with ROK inhibitor (Y27632 or H1152) for 15 min prior to two additional contraction-relaxation cycles in the continued presence of inhibitor. The ROK inhibitor was then washed out and two control contraction-relaxation cycles recorded again. Representative data showing the effects of H1152 on these contractile responses are shown in Fig. 1*A* with cumulative quantitative data for both inhibitors in Fig. 1*B*. The contractile responses to EFS, KCl or phenylephrine were all markedly inhibited by both ROK inhibitors (Fig. 1*A,B*). Furthermore, inhibition of ROK during steady-state force maintenance in the presence of phenylephrine elicited relaxation (Fig. 1*C*). The general protein kinase C (PKC) inhibitor, GF109203X, on the other hand, had no significant effect on the contractile response of the urethra to any of the stimuli (Supplementary Fig. 1). The efficacy of the PKC inhibitor was verified by its ability to block the contractile response of the rabbit urethra to 0.5 μM phorbol 12,13-dibutyrate (PdBu): steady-state force in response to 0.5 μM PdBu (0.47 ± 0.13 g) was reduced to 0.20 ± 0.09 g (n = 6; $p < 0.01$) following pre-incubation with 2 μM GF109203X. It is noteworthy that the contractile response to PdBu was very slow and reached a steady-state level of force that was much less than that induced by KCl or phenylephrine.

In order to pursue the mechanism underlying the contractile responses and the effects of ROK inhibition shown in Fig. 1, it was necessary to use an experimental system that is amenable to rapid quenching for biochemical analysis. For this purpose, urethral muscle strips were mounted in a 1-ml cuvette at room temperature and the effects of ROK inhibition on phenylephrine- and KCl-induced contraction examined. Fig. 2*A* shows the inhibition of phenylephrine-induced contraction by H1152 (1 μM): the mean maximal tension in response to phenylephrine in the presence of H1152 was 56.8% of control, compared to 118% of control following washout of the ROK inhibitor. The concentration dependence of H1152-induced relaxation of tissue pre-contracted with phenylephrine is shown in Fig. 2*B*. Additional experiments in which longer time intervals were used between successive additions of

H1152 indicated that the concentration required for half-maximal relaxation was 0.3 μM H1152 (Fig. 2*C*). H1152 had a similar inhibitory effect on KCl-induced contraction under these conditions (data not shown).

These results indicate that contraction of rabbit urethral smooth muscle evoked by EFS, membrane depolarization or α_1-adrenoceptor activation involves activation of ROK, but not PKC, and suggest that contraction of the urethra may involve a significant Ca^{2+} sensitization. Activation of ROK has been implicated in the inhibition of MLCP through the phosphorylation of MYPT1 at T697 and/or T855 (16,31,39). ROK is also known to phosphorylate CPI-17 at T38, which converts it into a potent inhibitor of MLCP (27). Inhibition of MLCP activity would shift the kinase-phosphatase activity balance in favour of MLCK and therefore increase LC_{20} phosphorylation and force.

LC_{20} phosphorylation. To initiate the investigation of the mechanism whereby ROK regulates urethral smooth muscle contraction, we measured LC_{20} phosphorylation levels in extracts of tissues quenched at rest and at the peak of contraction induced by phenylephrine or KCl. Phosphorylated and unphosphorylated LC_{20} were separated by Phos-tag SDS-PAGE and detected by western blotting with an antibody that recognizes both forms of the light chain (Fig. 3*A*): LC_{20} was phosphorylated to ~0.6 mol P_i/mol LC_{20} at resting tension (lanes 5 and 6). Western blotting with a phosphospecific antibody that recognizes only LC_{20} phosphorylated at S19, the MLCK site (Fig. 3*B*), and Phos-tag SDS-PAGE in the presence of EDTA to chelate Mn^{2+} ions (Fig. 3*C*), confirmed the identities of the bands as labelled. Thus, only the slower migrating band was recognized by the phosphospecific antibody (Fig. 3*B*) and, when Mn^{2+} ions were chelated with EDTA, LC_{20} migrated as a single band with the mobility of unphosphorylated LC_{20} observed in the presence of Mn^{2+} (Fig. 3*C*). Surprisingly, treatment with phenylephrine (Fig. 3*A*, lanes 1 and 2) or KCl (Fig. 3*A*, lanes 8 and 9) did not increase the level of LC_{20} phosphorylation. The cumulative quantitative data in Table 1 confirm this conclusion. Also shown in

Fig. 3*A* (lanes 3 and 4) is LC_{20} mono- and diphosphorylation (S19 and T18) in rabbit urethral smooth muscle strips contracted in response to the phosphatase inhibitor, calyculin-A. No LC_{20} diphosphorylation was detected in response to phenylephrine or KCl (Fig. 3*B*). Pre-incubation with H1152 had no effect on LC_{20} phosphorylation in the presence of KCl or phenylephrine (Fig. 3*D* and Table 1).

The possibility arose that because LC_{20} phosphorylation was quantified after steady-state force was achieved, a transient increase in LC_{20} phosphorylation correlating with force development may have been missed. Therefore, the time courses of LC_{20} phosphorylation in response to treatment with KCl and phenylephrine were investigated. Fig. 4 shows that there was, in fact, no change in LC_{20} phosphorylation throughout the time course of KCl- or phenylephrine-induced contraction.

MYPT1 phosphorylation. Since MYPT1 is a well known substrate of ROK in various smooth muscles, we examined the phosphorylation of MYPT1 at the two ROK sites by western blotting with phosphospecific antibodies. Both sites were phosphorylated at resting tension and neither KCl nor phenylephrine changed the level of phosphorylation at either site at the peak of the contractile response (Fig. 5 and Table 2). Analysis of the time course of phosphorylation revealed that MYPT1 phosphorylation at T697 and T855 did not change during the contraction elicited by either KCl (Fig. 6*A* and *C*) or phenylephrine (Fig. 6*B* and *C*). In order to determine whether T697 and T855 were stoichiometrically or only partially phosphorylated, MYPT1 phosphorylation in intact rabbit urethral strips treated with KCl was compared with Triton-skinned tissues treated with the phosphatase inhibitor microcystin. Resting levels of MYPT1 phosphorylation at T697 and T855 were unaffected by KCl treatment of intact tissues, whereas substantial increases in phosphorylation at both sites occurred upon treatment of the demembranated tissue with microcystin (Fig. 7). Densitometric analysis of the western blots gave a ratio of KCl:control signals (normalized to calponin) of 1.03 ± 0.13 and 0.79 ± 0.21 (mean

± SEM, n = 3) for T697 and T855, respectively, and a ratio of microcystin:control of 2.03 ± 0.08 and 8.78 ± 1.00 (mean ± SEM, n = 3) for T697 and T855, respectively.

CPI-17. Although CPI-17 is well established as a PKC substrate (24,27), it has also been implicated as a ROK substrate, at least *in vitro* (15,25). Phosphorylation by both kinases occurs at T38 and renders CPI-17 a potent MLCP inhibitor. Therefore, we investigated the expression of CPI-17 in the rabbit urethra. Consistent with previous findings with non-vascular smooth muscles (43), the level of CPI-17 in the urethra is considerably less than in vascular smooth muscles and comparable to the level in bladder (Supplementary Fig. 2). Given the low tissue content of CPI-17, the fact that LC_{20} phosphorylation was unaffected by ROK inhibition (Fig. 3*D* and Table 1) and the lack of effect of PKC inhibition on urethral contractility (Supplementary Fig. 1), we decided not to pursue the analysis of CPI-17 phosphorylation.

Cofilin phosphorylation. LIM kinase (10) has also been shown to be a ROK substrate, and phosphorylation at T508 within the activation loop activates this kinase (32). Activated LIM kinase in turn phosphorylates the actin capping and severing protein, cofilin, at S3 (7,44). In the unphosphorylated state, cofilin binds to and severs actin filaments and this effect is alleviated upon phosphorylation at S3 (1). We examined the time course of cofilin phosphorylation in rabbit urethral smooth muscle in response to KCl and phenylephrine by western blotting with a phosphospecific antibody that recognizes cofilin only when phosphorylated at S3. As shown in Fig. 8, cofilin is phosphorylated at S3 in the unstimulated tissue and its phosphorylation level does not change significantly during the time course of contraction in response to either KCl or phenylephrine.

Actin polymerization. We also measured actin polymerization during the time course of the contractile response to KCl and phenylephrine. Urethral tissue strips were homogenized in F-actin stabilization solution at the times indicated in Fig. 4*A* and *B*, and F- and G-actin were separated by high-speed centrifugation. Fig. 9*A* demonstrates that SM-22, a 22 kDa smooth muscle-specific protein (30), was

recovered exclusively in the high-speed supernatant and, therefore, provides a suitable protein for normalization of loading levels. The high-speed supernatant, containing all the G-actin, was then analysed by western blotting with anti-actin and loading levels were normalized to SM-22 (Fig. 9*B*). If KCl and phenylephrine induce actin polymerization that is required for force production in the urethra, we would anticipate that the G-actin content would decline rapidly in response to both stimuli and would increase again during relaxation upon washout. This was not found to be the case (Fig. 9*B*).

Comparison of LC_{20} phosphorylation in rabbit urethra, bladder and aorta. The very high level of basal phosphorylation of LC_{20} in the rabbit urethra at resting tension (0.65 mol P_i/mol LC_{20}) was unexpected, as was the absence of an increase in response to membrane depolarization or α_1-adrenoceptor activation (Table 1). Therefore, we investigated whether the same was true for another phasic urogenital smooth muscle (bladder) and a tonic vascular smooth muscle (aorta). As for the urethra, the basal level of LC_{20} phosphorylation in bladder smooth muscle was high and did not significantly change in response to KCl or phenylephrine (Table 3). On the other hand, the basal level of LC_{20} phosphorylation in the aorta was lower and did increase in response to both KCl and phenylephrine (Table 3).

LC_{20} phosphorylation in rat urethra and bladder. The role of LC_{20} phosphorylation in contraction of urethra and bladder smooth muscles was also investigated in rat tissues. In contrast to the situation with rabbit tissues, LC_{20} phosphorylation in rat urethra and bladder was relatively low at resting tension and increased in response to both KCl and phenylephrine (Table 4).

Comparison of methods for quenching of tissues prior to LC_{20} phosphorylation analysis. During the course of this work, we discovered that the method for quenching of rabbit urethral smooth muscle strips for biochemical analysis was crucial. This is often achieved by immersing the tissue in TCA/acetone/DTT on dry ice or clamping the tissue between liquid nitrogen-cooled tongs, immersing it

in TCA/acetone/DTT on dry ice and slowly warming the tissue to room temperature in TCA/acetone/DTT. However, we found that these procedures resulted in very low levels of LC_{20} phosphorylation (Table 5). On the other hand, immersing the tissue in TCA/acetone/DTT on wet ice gave much higher and reproducible phosphorylation stoichiometry (Table 1). We also quenched the tissues by immersion in liquid nitrogen, followed by transfer directly to boiling SDS-gel sample buffer. After incubation at 95 ^{o}C for 10 min, samples were rotated overnight at 4 ^{o}C prior to Phos-tag SDS-PAGE. As shown in Supplementary Figure 3 and Supplementary Table 1, very low levels of LC_{20} phosphorylation stoichiometry were measured under these conditions. In addition, rabbit urethral smooth muscle strips were clamped between liquid nitrogen-cooled tongs at rest and at the plateau of KCl- or phenylephrine-induced contractions and then treated in one of the following ways: (i) tissues were immersed in TCA/acetone/DTT on wet ice; (ii) tissues were immersed in TCA/acetone/DTT on dry ice; or (iii) tissues were immersed in liquid N_2. Tissues from (i) and (ii) were then lyophilized overnight after washing with acetone/DTT. All three sets of tissues were then immersed in boiling SDS-gel sample buffer, maintained at 95 ^{o}C for 10 min, and rotated at 4 ^{o}C overnight prior to Phos-tag SDS-PAGE to quantify LC_{20} phosphorylation levels. The results confirmed a high level of resting LC_{20} phosphorylation when tissues freeze-clamped with liquid N_2-cooled tongs were immersed in TCA/acetone/DTT on wet ice (Supplementary Table 2). On the other hand, much lower levels of LC_{20} phosphorylation were measured when tissues freeze-clamped with liquid N_2-cooled tongs were immersed in TCA/acetone/DTT on dry ice. Even lower levels of LC_{20} phosphorylation were measured when tissues freeze-clamped with liquid N_2-cooled tongs were immersed in liquid N_2.

The effects of removal of extracellular Ca^{2+} and pre-incubation with wortmannin on rabbit urethral smooth muscle contraction and LC_{20} phosphorylation. Finally, to identify the kinase responsible for the high level of LC_{20} phosphorylation in the rabbit urethra under resting conditions, the effect on LC_{20}

phosphorylation of removal of extracellular Ca^{2+} and pre-incubation with wortmannin (10 μM), which at this concentration is a MLCK inhibitor, was investigated. Incubation of urethral tissue strips in Ca^{2+}-free Krebs solution containing 10 mM EGTA for 30 min resulted in a marked decrease in LC_{20} phosphorylation and resting tension (Table 6). Treatment with KCl (80 mM) or phenylephrine (10 μM) after pre-incubation of tissue strips in Ca^{2+}-free Krebs solution containing 10 mM EGTA for 30 min failed to elicit a contractile response or an increase in LC_{20} phosphorylation (Table 6). Preincubation of tissue strips with wortmannin (10 μM) in Krebs solution also reduced the resting level of LC_{20} phosphorylation and reduced resting tension by over 50% (Table 6). Addition of KCl (80 mM) after incubation with wortmannin for 30 min failed to elicit a contractile response or an increase in LC_{20} phosphorylation (Table 6).

DISCUSSION

The most interesting findings from this study were that the urethra and bladder of the rabbit had a high level of LC_{20} phosphorylation at resting tension, and that membrane depolarization and α_1-adrenoceptor stimulation did not increase the level of LC_{20} phosphorylation (Figs. 3 and 4 and Table 1), in spite of inducing robust contractile responses (Figs. 1 and 2). Vascular smooth muscle of the rabbit (aorta), on the other hand, behaved as expected, i.e., LC_{20} phosphorylation increased in response to membrane depolarization and α_1-adrenoceptor stimulation (Table 3). Rat urethra and bladder, however, had a low level of LC_{20} phosphorylation at rest, which increased in response to membrane depolarization and α_1-adrenoceptor stimulation, indicating species specificity (Table 4). It will be important in the future to determine whether human urethral and bladder smooth muscles behave like the rabbit or rat counterparts.

Another key finding from this study was that the contractile responses to electric field stimulation,

KCl and phenylephrine were all potently inhibited by Y27632 and H1152, two structurally unrelated inhibitors of ROK (Figs. 1 and 2). It is important to note that, although highly selective, these compounds can inhibit other kinases such as PRK2, AMPK and, to a lesser degree, PDK11 (9). PRK2 and PDK11 have not been implicated in the regulation of smooth muscle contraction and AMPK has been shown to phosphorylate and inactivate smooth muscle MLCK (20). Given our observation that Y27632 and H1152 had no effect on LC_{20} phosphorylation (Fig. 3*D* and Table 1), it is unlikely that the inhibitory effects of Y27632 and H1152 on contraction involve inhibition of AMPK.

The RhoA/ROK pathway has previously been implicated in agonist-induced contraction of the rat urethra (37) and spontaneous tone in female porcine urethral smooth muscle (28). Extensive studies of various smooth muscles have implicated the RhoA/ROK pathway in Ca^{2+} sensitization, i.e., an increase in force at a given $[Ca^{2+}]_i$. This pathway results in inhibition of MLCP via phosphorylation of the myosin targeting subunit of MLCP (MYPT1) and/or CPI-17 by ROK, which results in increased LC_{20} phosphorylation and contraction (33). Since ROK inhibition did not alter LC_{20} phosphorylation in rabbit urethral smooth muscle (Fig. 3 and Table 1), we concluded that MLCP inhibition is not involved in the contractile response to KCl or phenylephrine. This conclusion was supported by the fact that MYPT1 phosphorylation at the two inhibitory ROK sites did not increase in response to either stimulus (Figs. 5 and 6 and Table 2), although phosphorylation could be greatly enhanced by treatment with the phosphatase inhibitor, microcystin (Fig. 7), indicating that resting phosphorylation at T697 and T855 was sub-stoichiometric. We did not pursue the phosphorylation of CPI-17 since tissue levels of this protein were very low in comparison to vascular smooth muscles (Supplementary Fig. 2), consistent with reports in the literature that CPI-17 is most highly expressed in tonic vascular smooth muscles and least in phasic visceral smooth muscles (43), and PKC, which is known to phosphorylate CPI-17 at T38, is not involved in rabbit urethral smooth muscle contraction in response to electric field stimulation,

membrane depolarization or α_1-adrenoceptor stimulation (Supplementary Fig. 1). Furthermore, the fact that ROK inhibition had no effect on LC_{20} phosphorylation supports the conclusion that CPI-17 does not have a role in the contractile responses observed.

Another ROK substrate that may play a role in regulation of contractility is LIM kinase, which contains two LIM domains, zinc finger domains originally identified in the proteins Lin11, Isl-1 and Mec-3 (8). This kinase is activated by ROK-catalysed phosphorylation within the activation loop. The activated LIM kinase phosphorylates the actin capping and severing protein cofilin at S3, whereupon it loses the ability to bind to actin and sever actin filaments (10). Actin polymerization has been implicated in smooth muscle contraction, and dephosphorylation of cofilin at S3 favors actin polymerization by increasing the availability of barbed ends of actin filaments (17). This would predict that dephosphorylation of cofilin, and not ROK/LIM kinase-mediated phosphorylation at S3 would occur in response to contractile stimulation, and a decrease in phosphocofilin has been demonstrated in canine tracheal smooth muscle treated with acetylcholine or KCl, which is associated with actin polymerization and contraction (45). Nevertheless, we investigated cofilin phosphorylation in rabbit urethral smooth muscle. While cofilin exhibited a basal level of S3 phosphorylation under resting tension, there was no change in cofilin phosphorylation in response to membrane depolarization or α_1-adrenoceptor stimulation (Fig. 8). Furthermore, there was no change in G-actin content in response to KCl or phenylephrine (Fig. 9). We concluded, therefore, that the ROK/LIM kinase/cofilin pathway is not responsible for membrane depolarization- or α_1-adrenoceptor stimulation-induced contraction of rabbit urethral smooth muscle.

The phosphatase inhibitor calyculin-A induced diphosphorylation of LC_{20} (Fig. 3*A* and *B*) and contraction of intact urethral smooth muscle (data not shown). We have shown previously that LC_{20} diphosphorylation occurs at S19 and T18 in vascular smooth muscle, and is catalysed by integrin-linked

kinase, not MLCK (14,40). We did not observe any LC_{20} diphosphorylation in urethral smooth muscle under resting conditions or in response to KCl or phenylephrine (e.g., Fig. 3) and conclude that ILK is not responsible for the high level of LC_{20} phosphorylation observed at rest or in the presence of these contractile stimuli. ROK has been shown to phosphorylate LC_{20} directly *in vitro*, although this does not appear to occur *in situ* (34). The fact that ROK inhibition by H1152 had no effect on LC_{20} phosphorylation under resting conditions or in the presence of KCl or phenylephrine (Fig. *3D* and Table 1) indicates that ROK is not responsible for the observed phosphorylation of LC_{20}. At resting tension, LC_{20} phosphorylation was almost abolished by removal of extracellular Ca^{2+} or by addition of wortmannin (MLCK inhibitor) in the presence of 2.5 mM extracellular Ca^{2+} (Table 6). Furthermore, KCl and phenylephrine failed to elicit a contractile response in the absence of extracellular Ca^{2+} or in the presence of wortmannin at 2.5 mM extracellular Ca^{2+} (Table 6). These results indicate that MLCK is the kinase responsible for LC_{20} phosphorylation in the rabbit urethra at rest and in the presence of KCl and phenylephrine.

The method used to quench the urethral tissue strips for biochemical analysis proved crucial. If tissues were immersed in TCA/acetone/DTT on dry ice, or clamped between liquid nitrogen-cooled tongs prior to immersion in TCA/acetone/DTT on dry ice and gradual warming to room temperature, the levels of LC_{20} phosphorylation were consistently very low at rest and did not change in response to KCl or phenylephrine (Table 5). On the other hand, if tissues were immersed in TCA/acetone/DTT on wet ice, the levels of LC_{20} phosphorylation were consistently much higher at rest, and again did not change in response to KCl or phenylephrine (Table 1). These results suggest that the use of TCA/acetone/DTT on dry ice does not rapidly quench cellular biochemical reactions so that LC_{20} is dephosphorylated by MLCP that remains active under these conditions. If the tissue was freeze-clamped between liquid nitrogen-cooled tongs, and subsequently immersed in TCA/acetone/DTT on wet ice or dry ice, or in

liquid nitrogen, differences in LC_{20} phosphorylation levels were again observed (Table 5 and Supplementary Table 2). In the case of immersion in wet ice-cooled TCA/acetone/DTT, resting LC_{20} stoichiometry was 0.36 mol P_i/mol LC_{20}, which did not change in response to contractile stimuli (Supplementary Table 2). On the other hand, very low levels of LC_{20} phosphorylation were measured in the cases of tissues that had been freeze-clamped between liquid nitrogen-cooled tongs and then immersed in dry-ice-cooled TCA/acetone/DTT or liquid nitrogen. Furthermore, for tissues that were immersed directly in liquid nitrogen and then transferred to boiling SDS-gel sample buffer, the measured stoichiometry of LC_{20} phosphorylation was again very low (Supplementary Fig. 3 and Supplementary Table 1), consistent with a very high tissue phosphatase activity. We interpret these results as follows: freeze-clamping the tissue between liquid nitrogen-cooled tongs, or plunging the tissue in liquid nitrogen or dry ice-cooled TCA/acetone/DTT dramatically reduces the phosphatase activity, but as the tissue warms up in SDS-gel sample buffer or TCA/acetone/DTT the phosphatase becomes active again and dephosphorylates LC_{20} before a sufficiently high temperature is reached to denature the phosphatase. It appears unlikely that immersion of tissue in wet ice-cooled TCA/acetone/DTT would lead to activation of MLCK since the kinase requires Ca^{2+}, Mg^{2+} and ATP for activity and none are present in the quench solution. Our observation that immersion of unstimulated rat tissues in wet ice-cooled TCA/acetone/DTT gave the expected low basal levels of LC_{20} phosphorylation also argues against activation of MLCK under these quenching conditions. It is also clear from the results presented that any manipulation involving rapid freezing of the rabbit urethra results in low levels of LC_{20} phosphorylation under both resting and stimulated conditions. In particular, it is apparent from Supplementary Table 2 that freeze-clamping the tissue with liquid nitrogen-cooled tongs followed by immersion in wet ice-cooled TCA/acetone/DTT yields lower and more variable LC_{20} phosphorylation stoichiometry (0.36 ± 0.07 mol P_i/mol LC_{20}) than direct immersion in wet ice-cooled

TCA/acetone/DTT (0.65 ± 0.02 mol P_i/mol LC_{20}), consistent with phosphatase activity dephosphorylating LC_{20} during sample work-up. Furthermore, we compared the basal level of LC_{20} phosphorylation at 0.5 g resting tension with that when no tension was applied to the tissue, and found no statistically significant difference by Student's t-test ($p > 0.05$): 0.66 ± 0.03 (n = 18) and 0.71 ± 0.11 (n = 10) mol P_i/mol LC_{20}, respectively. Also, if tissue at zero tension was quenched with dry ice-cooled TCA/acetone/DTT, low levels of LC_{20} phosphorylation were measured (0.11 ± 0.05 mol P_i/mol LC_{20}; n = 6). Caution must, therefore, be exercised when choosing a method of tissue quenching for quantification of LC_{20} phosphorylation in rabbit tissues.

Future studies will be directed towards identification of ROK substrates in rabbit urethra with a view to defining the mechanism of activation of contraction without an increase in LC_{20} phosphorylation.

ACKNOWLEDGEMENTS

The authors are grateful to Lada Abdrakhmanova, Andrew De Faoite, Cindy Sutherland and Emma J. Walsh for expert technical support. M.P.W. is an Alberta Heritage Foundation for Medical Research Scientist and recipient of a Canada Research Chair (Tier 1) in Vascular Smooth Muscle Research. W.C.C. is the Andrew Family Professor of Cardiovascular Research.

GRANTS

This research was supported by a grant from the Canadian Institutes of Health Research (MT13101) and a Science Foundation Ireland WTS Walton Award (to M.P.W.).

DISCLOSURES

No conflicts of interest are declared by the authors.

REFERENCES

1. **Agnew BJ, Minamide LS, Bamburg JR.** Reactivation of phosphorylated actin depolymerizing factor and identification of the regulatory site. *J Biol Chem* 270: 17582-17587, 1995.

2. **Allen BG, Walsh MP.** The biochemical basis of the regulation of smooth-muscle contraction. *Trends Biochem Sci* 19: 362-368, 1994.

3. **Andersson KE.** Pharmacology of lower urinary tract smooth muscles and penile erectile tissues. *Pharmacol Rev* 45: 253-308, 1993.

4. **Andersson KE.** Neurotransmission and drug effects in urethral smooth muscle. *Scand J Urol Nephrol Suppl* 207: 26-34, 2001.

5. **Andersson KE, Persson K.** The L-arginine/nitric oxide pathway and non-adrenergic, non-cholinergic relaxation of the lower urinary tract. *Gen Pharmacol* 24: 833-839, 1993.

6. **Andersson KE, Appell R, Awad S, Chapple C, Drutz H, Fourcroy J, Finkbeiner AE, Haab F, Wein A.** In *Incontinence, 1st International Consultation on Incontinence*. (Abrams, P., Khoury, S. and Wein, A., eds.), Plymbridge Distributors Ltd., Plymouth, U.K., 2002, pp. 479-512.

7. **Arber S, Barbayannis FA, Hanser H, Schneider C, Stanyon CA, Bernard O, Caroni P.** Regulation of actin dynamics through phosphorylation of cofilin by LIM-kinase. *Nature* 393: 805-809, 1998.

8. **Bach I.** The LIM domain: regulation by association. *Mech Dev* 9: 5-17, 2000.

9. **Bain J, Plater L, Elliott M, Shpiro N, Hastie CJ, McLauchlan H, Klevernic I, Arthur JSC, Alessi D, Cohen P.** The selectivity of protein kinase inhibitors: a further update. *Biochem J* 408: 297-315, 2007.

10. **Bernard O.** Lim kinases, regulators of actin dynamics. *Int J Biochem Cell Biol* 39: 1071-1076, 2007.

11. **Burnett AL.** Nitric oxide control of lower genitourinary tract functions: a review. *Urology* 45: 1071-1083, 1995.

12. Conte B, Maggi CA, Parlani M, Lopez G, Manzini S, Giachetti A. Simultaneous recording of vesical and urethral pressure in urethane-anesthetized rats: effect of neuromuscular blocking agents on the activity of the external urethral sphincter. J Pharmacol Methods 26: 161-171, 1991.

13. **Creed KE, Oike M, Ito Y.** The electrical properties and responses to nerve stimulation of the proximal urethra of the male rabbit. *Br J Urol* 79: 543-553, 1997.

14. **Deng JT, Van Lierop JE, Sutherland C, Walsh MP.** Ca^{2+}-independent smooth muscle contraction. A novel function for integrin-linked kinase. *J Biol Chem* 276: 16365-16373, 2001.

15. **Deng JT, Sutherland C, Brautigan DL, Eto M, Walsh MP.** Phosphorylation of the myosin phosphatase inhibitors, CPI-17 and PHI-1, by integrin-linked kinase. *Biochem J* 367: 517-524, 2002.

16. **Feng J, Ito M, Ichikawa K, Isaka N, Nishikawa M, Hartshorne DJ, Nakano T.** Inhibitory phosphorylation site for Rho-associated kinase on smooth muscle myosin phosphatase. *J Biol Chem* 274: 37385-37390, 1999.

17. **Gunst SJ, Zhang W.** Actin cytoskeletal dynamics in smooth muscle: a new paradigm for the regulation of smooth muscle contraction. *Am J Physiol Cell Physiol* 295: C576-C587, 2008.

18. **Hartshorne DJ, Ito M, Erdődi F.** Roles of protein phosphatase type 1 in contractile functions: myosin phosphatase. *J Biol Chem* 279: 37211-37214, 2004.

19. **Herbison P, Hay-Smith J, Ellis G, Moore K.** Effectiveness of anticholinergic drugs compared with placebo in the treatment of overactive bladder: systematic review. *Br Med J* 326: 841-844, 2003.

20. Horman S, Morel N, Vertommen D, Hussain N, Neumann D, Beauloye C, El Najjar N, Forcet

C, Viollet B, Walsh MP, Hue L, Rider MH. AMP-activated protein kinase phosphorylates and desensitizes smooth muscle myosin light chain kinase. *J Biol Chem* 283: 18505-18512, 2008.

21. **Hypolite JA, DiSanto ME, Zheng Y, Chang S, Wein AJ, Chacko S.** Regional variation in myosin isoforms and phosphorylation at the resting tone in urinary bladder smooth muscle. *Am J Physiol Cell Physiol* 280: C254-C264, 2001.

22. **Kaneko T, Amano M, Maeda A, Goto H, Takahashi K, Ito M, Kaibuchi K.** Identification of calponin as a novel substrate of Rho-kinase. *Biochem Biophys Res Commun* 273: 110-116, 2000.

23. **Kinoshita E, Kinoshita-Kikuta E, Takiyama, K, Koike T.** Phosphate-binding tag, a new tool to visualize phosphorylated proteins. *Mol Cell Proteomics* 5: 749-757, 2006.

24. **Kitazawa T, Takizawa N, Ikebe M, Eto M.** Reconstitution of protein kinase C-induced contractile Ca^{2+} sensitization in Triton X-100-demembranated rabbit arterial smooth muscle. *J Physiol* 520: 139-152, 1999.

25. **Koyama M, Ito M, Feng J, Seko T, Shiraki K, Takase K, Hartshorne DJ, Nakano T.** Phosphorylation of CPI-17, an inhibitory phosphoprotein of smooth muscle myosin phosphatase, by Rho-kinase. *FEBS Lett* 475: 197-200, 2000.

26. **Kumar V, Cross RL, Chess-Williams R, Chapple CR.** Recent advances in basic science for overactive bladder. *Curr Opin Urol* 15: 222-226, 2005.

27. **Li L, Eto M, Lee MR, Morita F, Yazawa M, Kitazawa T.** Possible involvement of the novel CPI-17 protein in protein kinase C signal transduction of rabbit arterial smooth muscle. *J Physiol* 508: 871-881, 1998.

28. **Malmqvist U, Hedlund P, Swärd K, Andersson KE.** Female pig urethral tone is dependent on Rho guanosine triphosphatases and Rho-associated kinase. *J Urol* 171: 1955-1958, 2004.

29. McHale NG, Hollywood MA, Sergeant GP, Shafel A, Thornbury KD, Ward SM. Organization

and function of ICC in the urinary tract. J Physiol 576: 689-694, 2006.

30. **Morgan KG, Gangopadhyay SS.** Cross-bridge regulation by thin filament-associated proteins. *J Appl Physiol* 91: 953-962, 2001.

31. **Murányi A, Derkach D, Erdődi F, Kiss A, Ito M, Hartshorne DJ.** Phosphorylation of Thr695 and Thr850 on the myosin phosphatase target subunit: Inhibitory effects and occurrence in A7r5 cells. *FEBS Lett* 579: 6611-6615, 2005.

32. **Ohashi K, Nagata K, Maekawa M, Ishizaki T, Narumiya S.** Rho-associated kinase ROCK activates LIM-kinase 1 by phosphorylation at threonine 508 within the activation loop. *J Biol Chem* 275: 3577-3582, 2000.

33. **Somlyo AP, Somlyo AV.** Ca^{2+} sensitivity of smooth muscle and nonmuscle myosin II: modulated by G proteins, kinases, and myosin phosphatase. *Physiol Rev* 83: 1325-1358, 2003.

34. **Swärd K, Dreja K, Susnjar M, Hellstrand P, Hartshorne DJ, Walsh MP.** Inhibition of Rho-associated kinase blocks agonist-induced Ca^{2+} sensitization of myosin phosphorylation and force in guinea pig ileum. *J Physiol* 522: 33-49, 2000.

35. **Takeya K, Loutzenhiser K, Shiraishi M, Loutzenhiser R, Walsh MP.** *Am J Physiol Renal Physiol* 294: F1487-F1492, 2008.

36. **Tanagho EA, Miller ER.** Initiation of voiding. *Br J Urol* 42: 175-183, 1970.

37. **Teixiera CE, Jin L, Priviero FBM, Ying Z, Webb RC.** Comparative pharmacological analysis of Rho-kinase inhibitors and identification of molecular components of Ca^{2+} sensitization in the rat lower urinary tract. *Biochem Pharmacol* 74: 647-658, 2007.

38. Thornbury KD, Hollywood MA, McHale NG. Mediation by nitric-oxide of neurogenic relaxation of the urinary-bladder neck muscle in sheep. *J Physiol* 451: 133-144, 1992.

39. **Velasco G, Armstrong C, Morrice N, Frame S, Cohen P.** (2002) Phosphorylation of the

590regulatory subunit of smooth muscle protein phosphatase 1M at Thr850 induces its dissociation from 591myosin. *FEBS Lett* 527: 101-104, 2002.

59240. **Weber LP, Van Lierop JE, Walsh MP.** Ca^{2+}-independent phosphorylation of myosin in rat caudal 593artery and chicken gizzard myofilaments. *J Physiol* 516: 805-824, 1999.

59441. **Wilson DP, Sutherland C, Walsh MP.** Ca^{2+} activation of smooth muscle contraction. Evidence for 595the involvement of calmodulin that is bound to the Triton-insoluble fraction even in the absence of Ca^{2+}. 596*J Biol Chem* 277: 2186-2192, 2002.

59742. **Winder SJ, Walsh MP.** Smooth muscle calponin. Inhibition of actomyosin MgATPase and 598regulation by phosphorylation. *J Biol Chem* 265: 10148-10155, 1990.

59943. **Woodsome TP, Eto M, Everett A, Brautigan DL, Kitazawa T.** Expression of CPI-17 and myosin 600phosphatase correlates with Ca(2+) sensitivity of protein kinase C-induced contraction in rabbit smooth 601muscle. *J Physiol* 535: 553-564, 2001.

60244. **Yang N, Higuchi O, Ohashi K, Nagata K, Wada A, Kangawa K, Nishida E, Mizuno K.** Cofilin 603phosphorylation by LIM-kinase 1 and its role in Rac-mediated actin reorganization. *Nature* 393: 809-604812, 1998.

60545. **Zhao R, Du L, Huang Y, Wu Y, Gunst SJ.** Actin depolymerization factor/cofilin activation 606regulates actin polymerization and tension development in canine tracheal smooth muscle. *J Biol Chem* 607283: 36522-36531, 2008.

608

Table 1 LC_{20} phosphorylation in rabbit urethral smooth muscle treated with KCl or phenylephrine, and the effect of ROK inhibition

Conditions	**mol P_i/mol LC_{20}**
Control	0.65 ± 0.02 (21)
KCl	0.63 ± 0.03 (22)
Phenylephrine	0.62 ± 0.03 (19)
H1152	0.55 ± 0.05 (7)
KCl + H1152	0.56 ± 0.03 (6)
Phenylephrine + H1152	0.57 ± 0.06 (7)

Rabbit urethral smooth muscle strips were treated with KCl, phenylephrine or vehicle with or without pre-incubation with the ROK inhibitor H1152 (see legend to Fig. 2). Tissues were immersed in TCA/acetone/DTT on wet ice at the peak of contraction, and LC_{20} phosphorylation was analysed by Phos-tag SDS-PAGE. Values indicate the mean ± SEM (*n* values given in parentheses). No significant differences from control were observed by one-way ANOVA with Dunnett's post-hoc test ($p > 0.05$).

620 *Table 2 MYPT1 phosphorylation in rabbit urethral smooth muscle treated with KCl or*
621 *phenylephrine*
622

Conditions	**pT697**	**pT855**
KCl	0.86 ± 0.09 (7)	0.88 ± 0.118 (7)
Phenylephrine	1.25 ± 0.21 (9)	1.38 ± 0.14 (9)

623

624Rabbit urethral smooth muscle strips were treated with KCl, phenylephrine, or vehicle (see legend to
625Fig. 2). Tissues were immersed in TCA/acetone/DTT on wet ice at the peak of contraction, and MYPT1
626phosphorylation at T697 and T855 was analysed by western blotting with phosphospecific antibodies.
627Values indicate signal intensities relative to control after normalization of loading levels ± SEM with *n*
628values in parentheses. No significant differences from control (set at a value of 1) were observed by
629Student's t test ($p > 0.05$).
630

Table 3 LC_{20} phosphorylation in rabbit urethral, bladder and aortic smooth muscles treated with KCL or phenylephrine

Conditions	**Urethra (mol P_i/molLC_{20})**	**Bladder (mol P_i/mol LC_{20})**	**Aorta (mol P_i/molLC_{20})**
Control	0.67 ± 0.07	0.63 ± 0.06	0.45 ± 0.05
KCl	0.70 ± 0.03	0.67 ± 0.01	0.59 ± 0.05*
Phenylephrine	0.70 ± 0.02	0.59 ± 0.06	0.65 ± 0.04*

Rabbit urethral, bladder and aortic smooth muscle strips were treated with KCl, phenylephrine, or vehicle (see legend to Fig. 2). Tissues were immersed in TCA/acetone/DTT on wet ice at the peak of contraction, and LC_{20} phosphorylation was analysed by Phos-tag SDS-PAGE. Values indicate the mean ± SEM (n = 6 for urethra, 3 for bladder and 5 for aorta). Statistically significant differences from control are indicated with asterisks (*$p < 0.05$) as determined by one-way ANOVA with Dunnett's post-hoc test.

643 *Table 4 LC_{20} phosphorylation in rat urethral and bladder smooth muscles treated with KCl or*
644 *phenylephrine*
645

Conditions	**Urethra (mol P_i/mol LC_{20})**	**Bladder (mol P_i/mol LC_{20})**
Control	0.13 ± 0.05	0.21 ± 0.06
KCl	0.37± 0.07*	0.43 ± 0.06*
Phenylephrine	0.41 ± 0.04**	0.45 ± 0.06*

646

647Rat urethral and bladder smooth muscle strips were treated with KCl, phenylephrine, or vehicle (see
648legend to Fig. 2). Tissues were immersed in TCA/acetone/DTT on wet ice at the peak of contraction,
649and LC_{20} phosphorylation was analysed by Phos-tag SDS-PAGE. Values indicate the mean ± SEM (n =
6504). Statistically significant differences from control are indicated with asterisks (*$p < 0.5$; **$p < 0.01$),
651as determined by one-way ANOVA with Dunnett's post-hoc test.
652

Table 5 LC_{20} phosphorylation in rabbit urethral smooth muscle treated with KCl or phenylephrine, and quenched in TCA/acetone/DTT on dry ice or clamped between liquid nitrogen-cooled tongs

Conditions	**Treatment (i) (mol P_i/mol LC_{20})**	**Treatment (ii) (mol P_i/mol LC_{20})**
Control	0.05 ± 0.01 (14)	0.04 ± 0.01 (3)
KCl	0.12 ± 0.03 (10)	0.07 ± 0.02 (3)
Phenylephrine	0.07 ± 0.02 (11)	0.04 ± 0.01 (3)

Rabbit urethral smooth muscle strips were treated with KCl, phenylephrine or vehicle (see legend to Fig. 2). (i) Tissues at the peak of contraction were immersed in TCA/acetone/DTT on dry ice, and then washed (3 x 1 ml) in acetone/DTT, the liquid poured off and the tissue lyophilized; or (ii) tissues at the peak of contraction were quick frozen by clamping between liquid nitrogen cooled tongs, immersed in TCA/acetone/DTT on dry ice, slowly (1 h) warmed to room temperature, washed (3 x 1 ml) in acetone/DTT, the liquid poured off and the tissue was frozen on dry ice and lyophilized. LC_{20} phosphorylation was analysed by Phos-tag SDS-PAGE. Values indicate the mean ± SEM (*n* values in parentheses). No statistically significant differences from control were detected by one-way ANOVA with Dunnett's post-hoc test ($p > 0.05$).

Table 6 The effects of removal of extracellular Ca^{2+} and pre-incubation with wortmannin on LC_{20} phosphorylation and contraction in rabbit urethral smooth muscle

Conditions	**mol P_i/mol LC_{20}**	**Contractile response**
Control	0.70 ± 0.02	None
0 Ca^{2+}	0.13 ± 0.08**	Relaxation (43.8 ± 5.8%)
KCl	0.66 ± 0.04	Contraction
0 Ca^{2+} + KCl	0.16 ± 0.03**	None
Phenylephrine	0.65 ± 0.05	Contraction
0 Ca^{2+} + phenylephrine	0.06 ± 0.04**	None
Wortmannin	0.16 ± 0.07**	Relaxation (52.8 ± 9.0%)
Wortmannin + KCl	0.06 ± 0.02**	None

Rabbit urethral smooth muscle strips were treated with KCl, phenylephrine or vehicle (see legend to Fig. 2) and the contractile responses were recorded. Tissues were immersed in TCA/acetone/DTT on wet ice, and LC_{20} phosphorylation was analysed by Phos-tag SDS-PAGE. Values indicate phosphorylation stoichiometry ± SEM (2 tissue strips from each of 2 animals were analysed in each case). Statistically significant differences from control, as indicated by one-way ANOVA with Dunnett's post-hoc test, are indicated with asterisks (**$p < 0.01$).

FIGURE LEGENDS

Fig. 1. Effects of ROK inhibition on urethral smooth muscle contraction. Rabbit urethral smooth muscle strips were dissected, mounted on a force transducer at resting tension and perfused with Krebs solution at 37 ^{o}C for at least 1 h. Two control contraction-relaxation cycles were recorded prior to incubation of the tissue with either H1152 (1 μM) or Y27632 (10 μM) for 15 min. Two contraction-relaxation cycles were recorded in the continued presence of inhibitor. The inhibitor was then washed out and two control contraction-relaxation cycles recorded again. *A*, representative traces depicting the effects of H1152 on contractions elicited by EFS (upper panel), KCl (middle panel) and phenylephrine (lower panel). *B*, cumulative data showing the effects of ROK inhibitors on contractions elicited by: electric field stimulation (EFS) at 4 Hz in the presence of H1152 (n = 6) or Y27632 (n = 8 with Y27632 and n = 6 following washout), KCl (80 mM) stimulation in the presence of H1152 (n = 5 with H1152 and n = 7 following washout) or Y27632 (n = 4), or phenylephrine (PHE; 10 μM) stimulation in the presence of H1152 (n = 6) or Y27632 (n = 9 with Y27632 and n = 8 following washout). Values indicate maximal tension as a percentage of the average tension of the initial control responses. Recovery (grey bars) indicates the average tension response following washout of the inhibitor (not significantly different from control). Statistically significant differences from control (absence of H1152), detected by one-way ANOVA with Dunnett's post-hoc test, are indicated by asterisks (**$p < 0.01$, n = 5). *C*, Effect of H1152 on sustained phenylephrine-induced contraction of urethral smooth muscle. Rabbit urethral smooth muscle strips equilibrated in Krebs solution at 37 ^{o}C were contracted with phenylephrine (10 μM). Following washout and relaxation, a sustained contractile response was elicited with phenylephrine. H1152 (1 μM) was added in the continued presence of phenylephrine, following which both phenylephrine and H1152 were washed out and a final control sustained contraction elicited with phenylephrine.

Fig. 2. Effect of H1152 on phenylephrine-induced contraction of non-perfused rabbit urethral smooth muscle strips at 21 ^{o}C. Rabbit urethral smooth muscle strips were dissected, mounted on a force transducer at resting tension and equilibrated with Krebs solution at 21 ^{o}C for at least 1 h. *A*, Two control phenylephrine (10 μM)-induced contraction-relaxation cycles were recorded prior to incubation of the tissue with H1152 (1 μM) for 15 min. Two contraction-relaxation cycles were recorded in the continued presence of inhibitor, which was then washed out and two control contraction-relaxation cycles recorded again. *B*, Following two control phenylephrine-induced contraction-relaxation cycles, phenylephrine was added again. The phenylephrine solution was changed 7 times and force was maintained. Following washout, another contraction was elicited by phenylephrine and increasing concentrations of H1152 (0.1, 0.25, 0.5, 1, 2.5, 5 and 10 μM) were applied in the continued presence of phenylephrine, followed by washout of phenylephrine and H1152. Although not clearly apparent in this figure, due to compression of the time scale, steady-state force was achieved before each addition of H1152, as seen on the expanded time scale of the recorder. *C*, Cumulative data showing the effects of increasing H1152 concentration on phenylephrine-induced contraction. In these experiments, longer time intervals were used between successive additions of H1152 than in panel *B* to ensure that steady-state force had been achieved.

Fig. 3. LC_{20} phosphorylation in rabbit urethral smooth muscle treated with phenylephrine or KCl, and the effect of ROK inhibition. Rabbit urethral smooth muscle strips were dissected, mounted on a force transducer at resting tension and equilibrated with Krebs solution at 21 ^{o}C for at least 1 h prior to treatment with phenylephrine (10 μM), KCl (80 mM), calyculin-A (5 μM) or vehicle (control). Tissues were quenched in TCA/DTT in acetone on wet ice once steady-state force was developed, washed with DTT in acetone and lyophilized overnight before extraction of tissue proteins with SDS-gel sample buffer. Phosphorylated and unphosphorylated forms of the 20 kDa myosin regulatory light chains (LC_{20})

were separated by SDS-PAGE (in duplicate) with polyacrylamide-bound Mn^{2+}-phosphate-binding tag (Phos-tag SDS-PAGE) and detected by western blotting with anti-LC_{20} (*A*) or phosphospecific anti-LC_{20}, which recognizes only LC_{20} phosphorylated at S19 (*B*). "LC_{20}" denotes unphosphorylated LC_{20}, "P_1-LC_{20}" denotes LC_{20} phosphorylated at S19 and "P_2-LC_{20}" denotes LC_{20} phosphorylated at S19 and T18. The position of the 28 kDa marker is indicated at the right. *C,* Triplicate samples of muscle strips treated with KCl (80 mM) or phenylephrine (10 μM) were subjected to Phos-tag SDS-PAGE in the presence of $MnCl_2$ (upper panel) or EDTA (lower panel). The position of the 26 kDa marker is indicated at the right. *D*, Rabbit urethral smooth muscle strips were pre-incubated with the ROK inhibitor H1152 (1 μM) prior to addition of phenylephrine (10 μM), KCl (80 mM) or vehicle. LC_{20} phosphorylation was analysed by Phos-tag SDS-PAGE. The position of the 28 kDa marker is indicated at the right.

Fig. 4. Time courses of LC_{20} phosphorylation in rabbit urethral smooth muscle treated with KCl or phenylephrine. Typical KCl (80 mM)- (*A*) and phenylephrine (10 μM)-induced (*B*) contractile responses. Numbers indicate the times during contractions at which tissues were quenched for Phos-tag SDS-PAGE analysis of LC_{20} phosphorylation (*C*). *D*, Cumulative data (values indicate the mean ± SEM, $n = 3$ for KCl and $n = 2$ for phenylephrine).

Fig. 5. MYPT1 phosphorylation in rabbit urethral smooth muscle treated with KCl or phenylephrine. Rabbit urethral smooth muscle strips were treated with phenylephrine (10 μM), KCl (80 mM) or vehicle (control) and the phosphorylation of MYPT1 at the peak of the contractile response was analysed in triplicate by western blotting with phosphospecific antibodies that recognize MYPT1 phosphorylated at T697 or T855. Loading levels were normalized to the actin-binding protein calponin.

Fig. 6. Time courses of MYPT1 phosphorylation in rabbit urethral smooth muscle treated with KCl or phenylephrine. Rabbit urethral smooth muscle strips were treated with 80 mM KCl (*A*) or 10 μM phenylephrine (*B*) and the phosphorylation of MYPT1 was analysed in triplicate at selected times during

the contractile response by western blotting with phosphospecific antibodies that recognize MYPT1 phosphorylated at T697 or T855. Loading levels were normalized to actin. Numbers beneath gel lanes indicate the times during contractions at which tissues were quenched for western analysis of MYPT1 phosphorylation (see Fig. 4*A* and *B*). *C*, Cumulative data (values indicate the mean ± SEM, $n = 4$ for KCl and $n = 3$ for phenylephrine).

Fig. 7. Phosphatase inhibition with microcystin markedly increases MYPT1 phosphorylation at T697 and T855. Rabbit urethral smooth muscle strips (intact or Triton-skinned) were treated with KCl (80 mM, intact strips), microcystin (10 μM, Triton-skinned strips) or vehicle (control, intact strips) and the phosphorylation of MYPT1 (130 kDa) analysed in triplicate by western blotting with phosphospecific antibodies. Loading levels were normalized to calponin (32 kDa). "M" denotes the molecular weight marker lane.

Fig. 8. Cofilin phosphorylation in rabbit urethral smooth muscle treated with KCl or phenylephrine. Rabbit urethral smooth muscle strips were treated with 80 mM KCl (*A*) or 10 μM phenylephrine (*C*) and the phosphorylation of cofilin was analysed at selected times during the contractile response by western blotting with phosphospecific antibodies that recognize cofilin phosphorylated at S3. Loading levels were normalized to LC_{20} and calponin. Numbers beneath gel lanes indicate the times during contractions at which tissues were quenched for analysis of cofilin phosphorylation (see Fig. 4*A* and *B*). *B* and *D*, Cumulative data for KCl- and phenylephrine-induced contractions, respectively (values indicate the mean ± SEM, $n = 4$ (*B*), $n = 3$ (*D*)).

Fig. 9. Analysis of actin polymerization during KCl- and phenylephrine-induced contraction of rabbit urethra. Rabbit urethral smooth muscle strips were treated with KCl (80 mM) or phenylephrine (10 μM). Tissues were homogenized, centrifuged at low speed to remove cell debris and then at high speed to separate F- and G-actin. The high-speed supernatants and pellets were analysed by western blotting with

anti-actin and anti-SM-22, and representative results are shown in *A*: lanes 1, 3, 6 and 8: KCl-treated tissues (15, 7.5, 7.5 and 15 µl, respectively); lanes 2, 4, 5 and 7: phenylephrine-treated tissues (15, 7.5, 7.5 and 15 µl, respectively). *B*, Tissues were homogenized at selected times during the contractions and centrifuged at high speed to remove F-actin. The high-speed supernatants were analysed by western blotting with anti-actin and anti-SM-22. Time courses in response to KCl or phenylephrine treatment are shown. Numbers beneath gel lanes in (*B*) indicate the times during contractions at which tissues were homogenized for western analysis of actin and SM-22 (see Fig. 4*A* and *B*).

FIGURE 1A

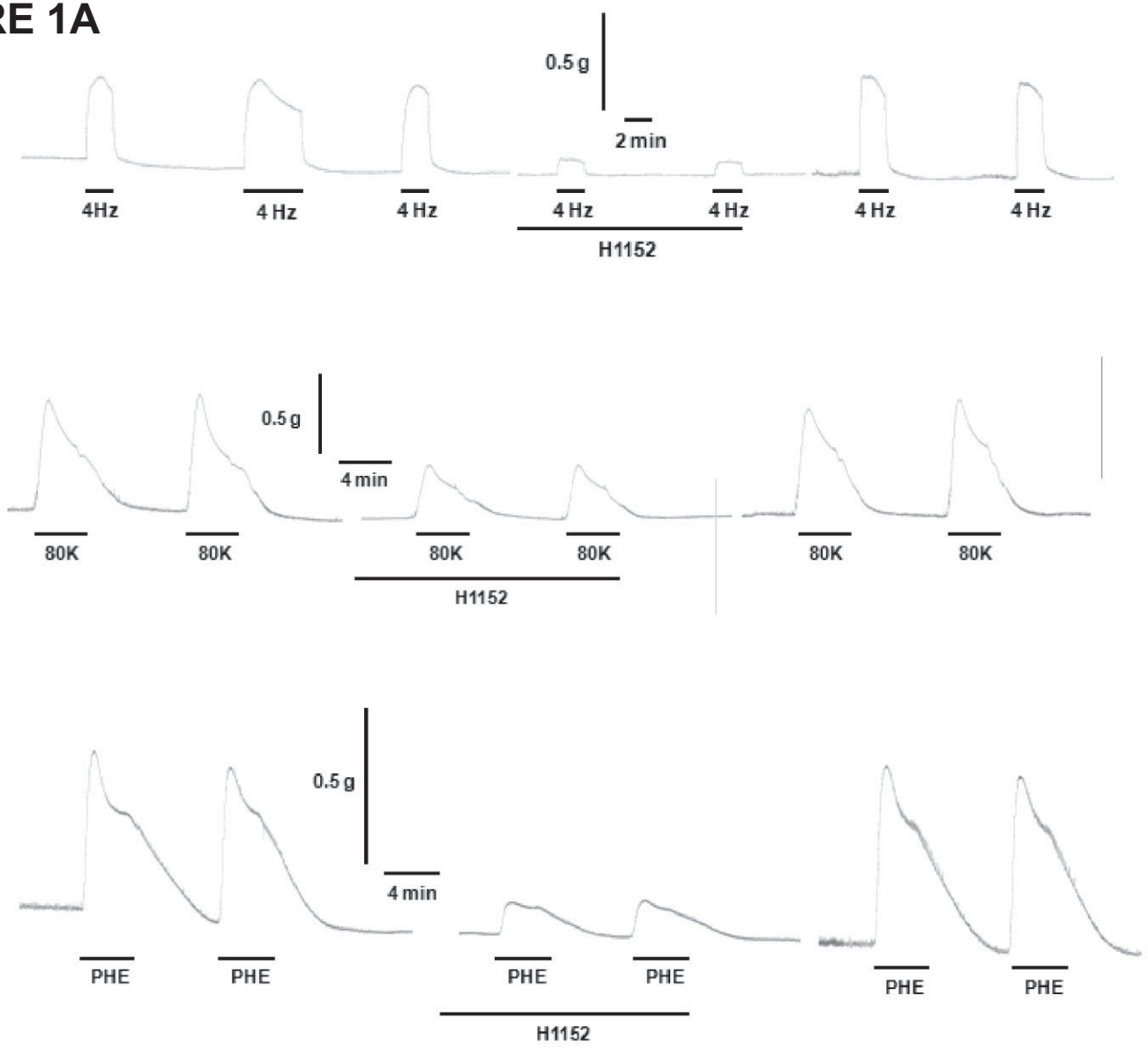
0.5 g
2 min
4Hz
4 Hz
4 Hz
4 Hz
4 Hz
4 Hz
4 Hz
H1152
0.5 g
4 min
80K
80K
80K
80K
80K
80K
H1152
0.5 g
4 min
PHE
PHE
PHE
PHE
PHE
PHE
H1152

FIGURE 1B

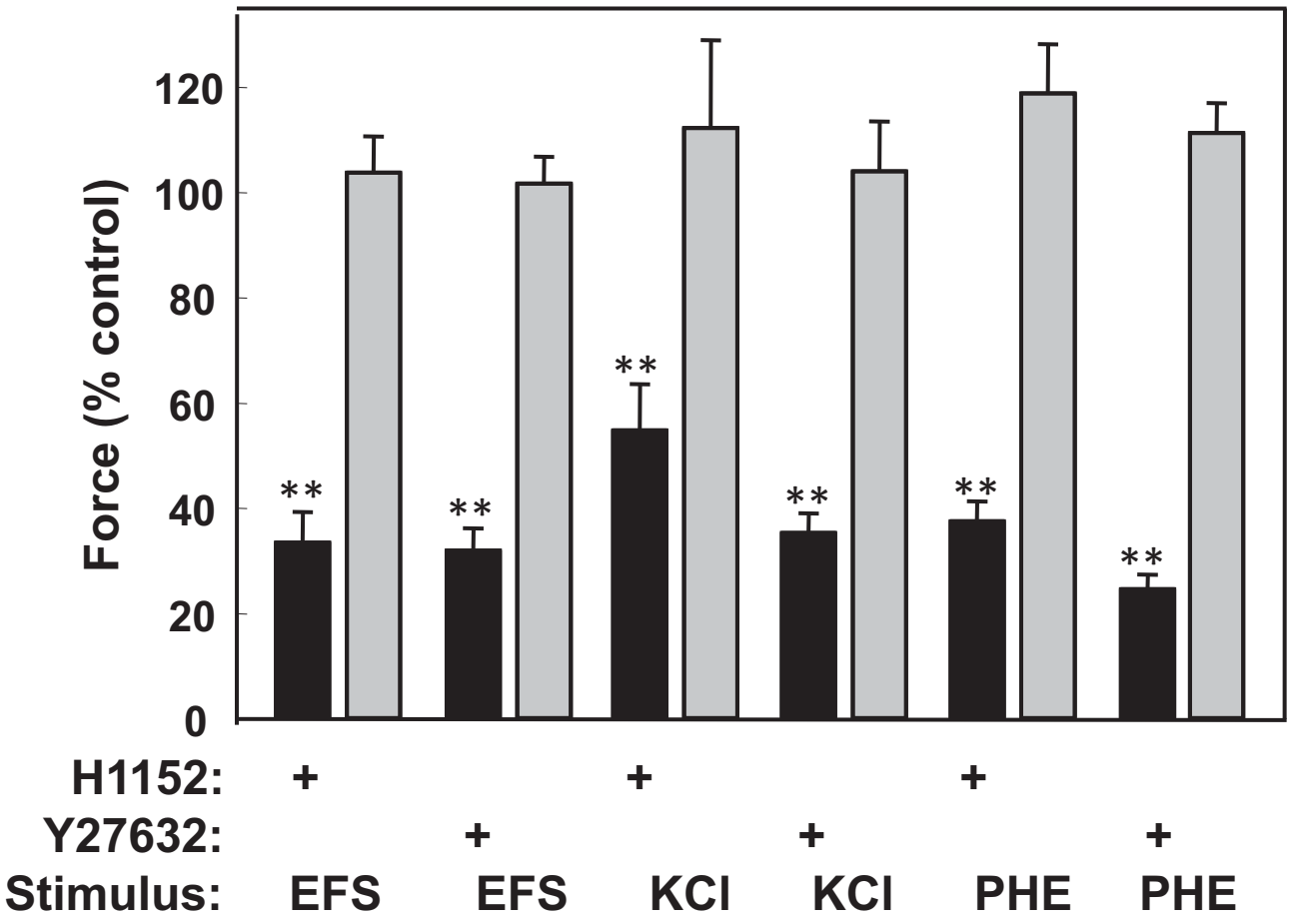
Force (% control)
120
100
80
60
40
20
0
**
**
**
**
**
**
H1152: + + +
Y27632: + + +
Stimulus: EFS EFS KCl KCl PHE PHE

FIGURE 1C

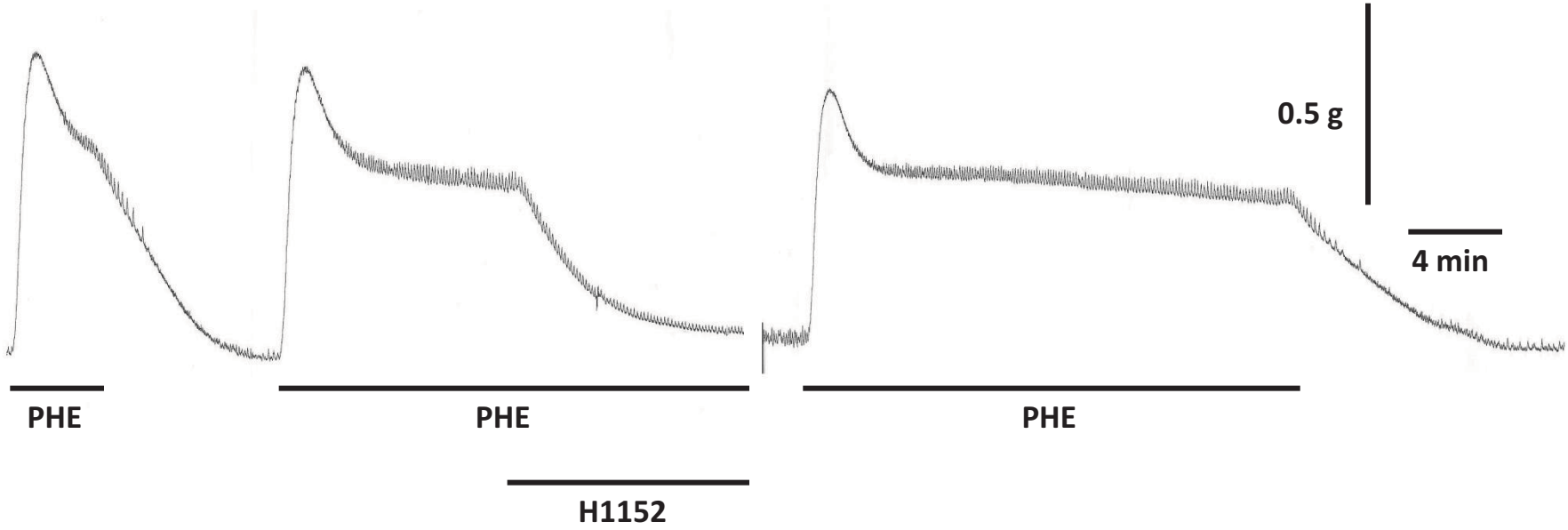

FIGURE 2A

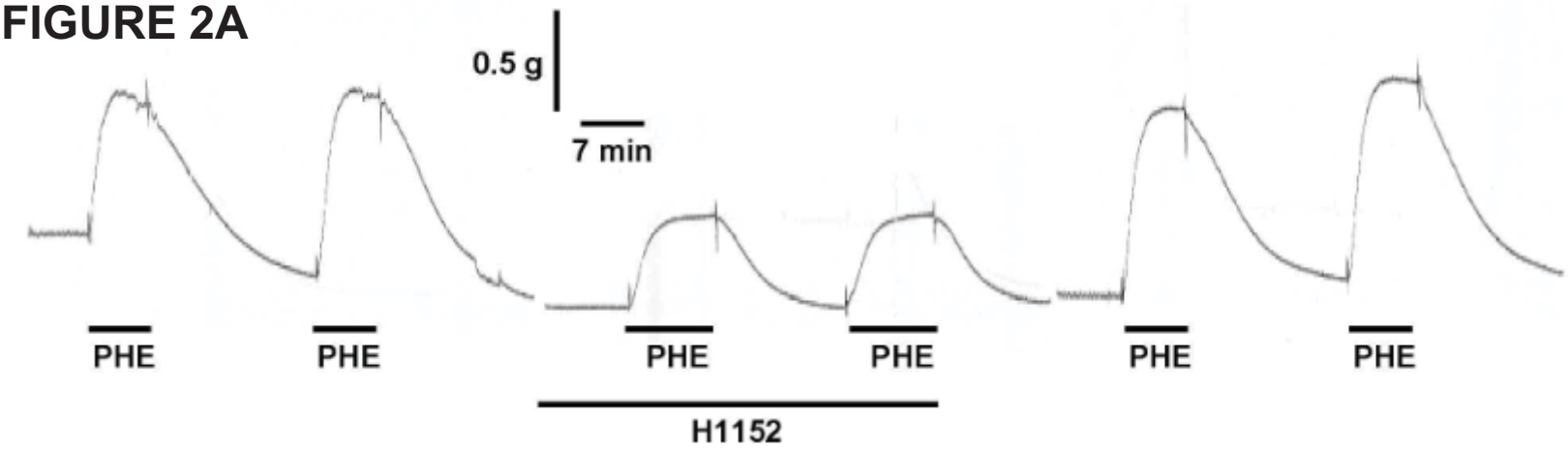

FIGURE 2B

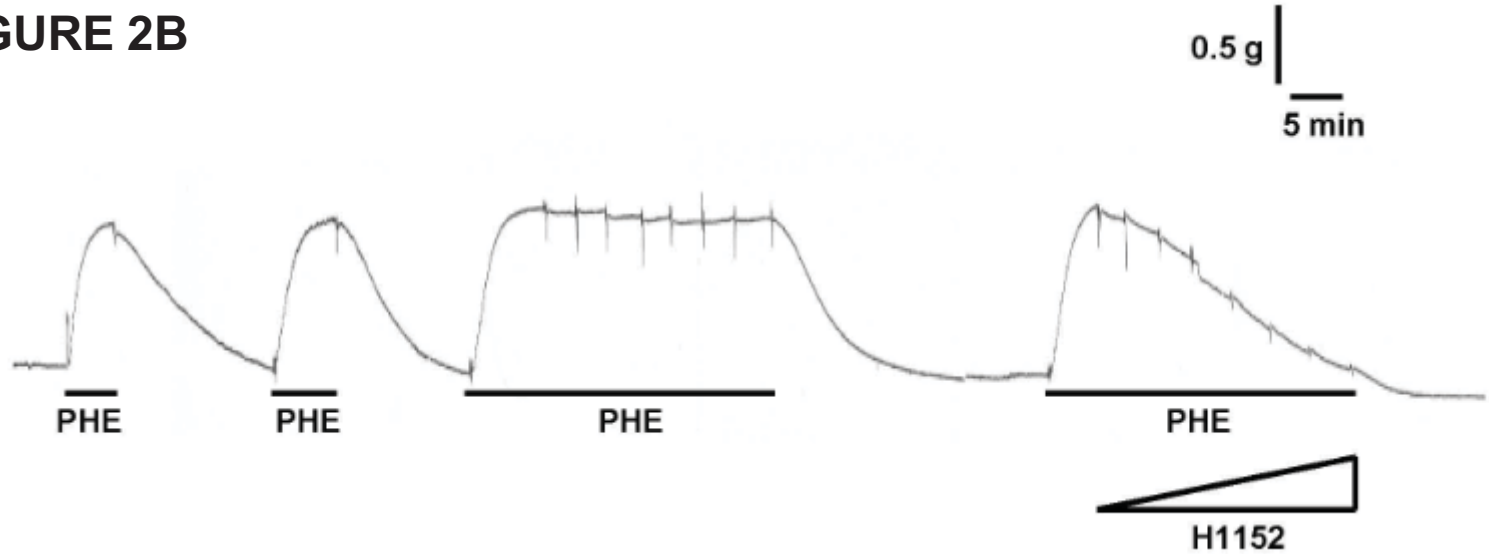

FIGURE 2C

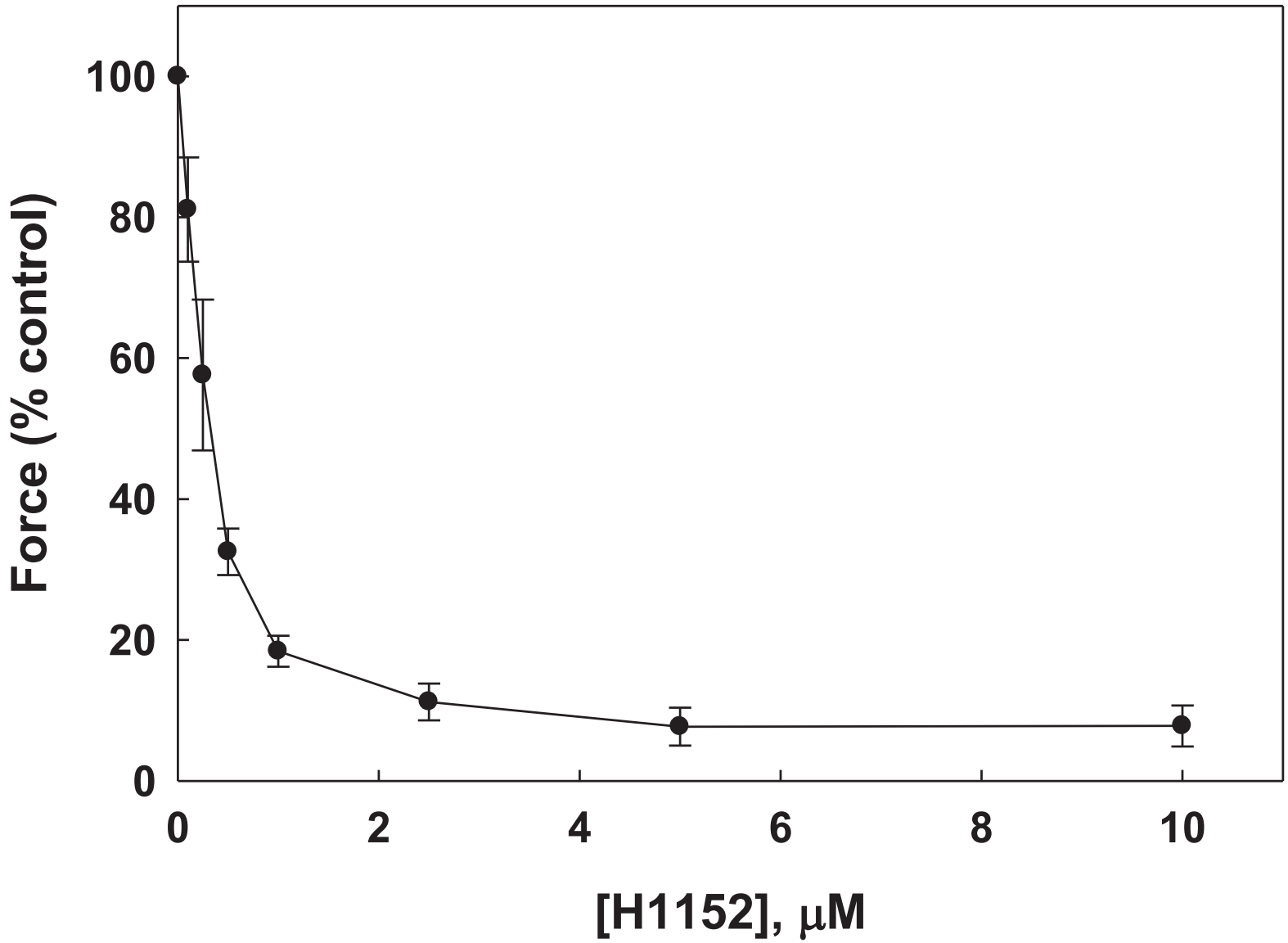

FIGURE 3

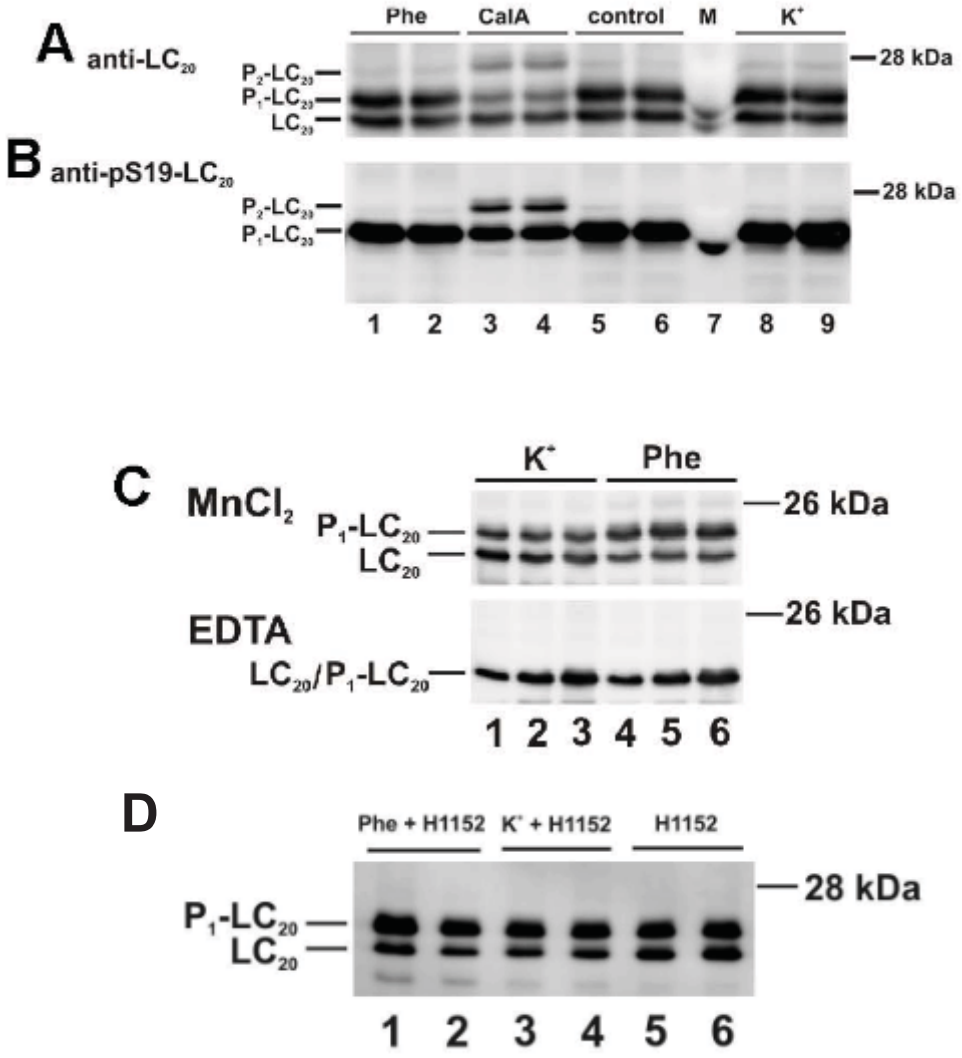
A
anti-LC20
Phe
CalA
control
M
K+
P2-LC20
P1-LC20
LC20
28 kDa
B
anti-pS19-LC20
P2-LC20
P1-LC20
28 kDa
1 2 3 4 5 6 7 8 9
C
MnCl2
K+
Phe
P1-LC20
LC20
26 kDa
EDTA
LC20/P1-LC20
26 kDa
1 2 3 4 5 6
D
Phe + H1152
K+ + H1152
H1152
P1-LC20
LC20
28 kDa
1 2 3 4 5 6

FIGURE 4

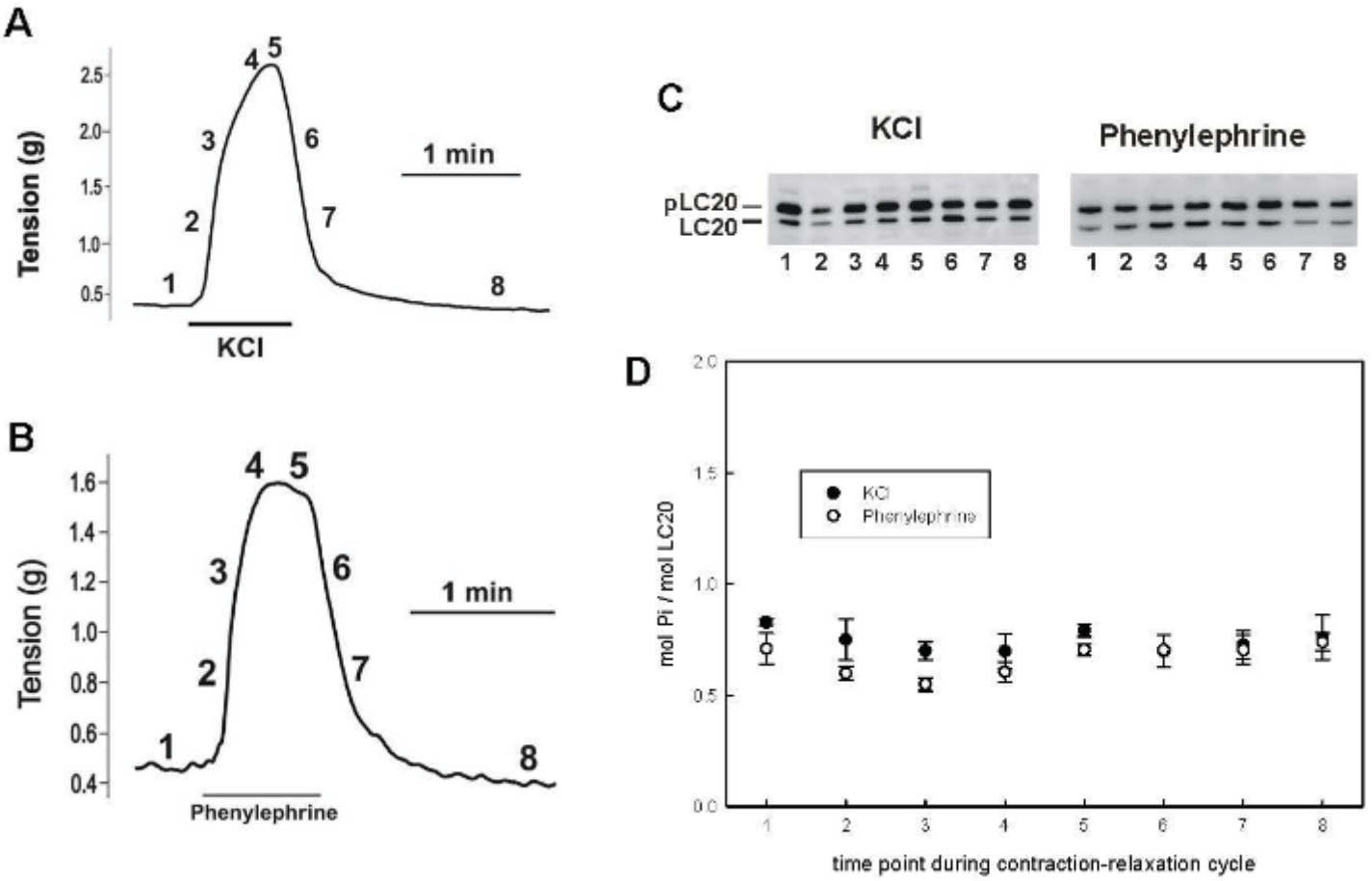
A
Tension (g)
2.5
2.0
1.5
1.0
0.5
1
2
3
4
5
6
7
8
1 min
KCl
B
Tension (g)
1.6
1.4
1.2
1.0
0.8
0.6
0.4
1
2
3
4
5
6
7
8
1 min
Phenylephrine
C
KCl
Phenylephrine
pLC20
LC20
1 2 3 4 5 6 7 8
1 2 3 4 5 6 7 8
D
mol Pi / mol LC20
2.0
1.5
1.0
0.5
0.0
KCl
Phenylephrine
1 2 3 4 5 6 7 8
time point during contraction-relaxation cycle

FIGURE 5

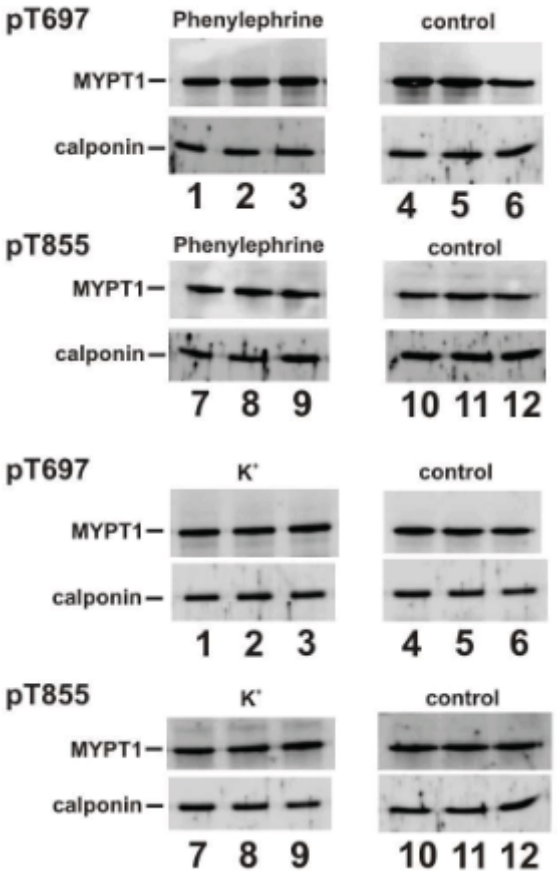
pT697
Phenylephrine
control
MYPT1
calponin
1 2 3
4 5 6
pT855
Phenylephrine
control
MYPT1
calponin
7 8 9
10 11 12
pT697
K+
control
MYPT1
calponin
1 2 3
4 5 6
pT855
K+
control
MYPT1
calponin
7 8 9
10 11 12

FIGURE 6

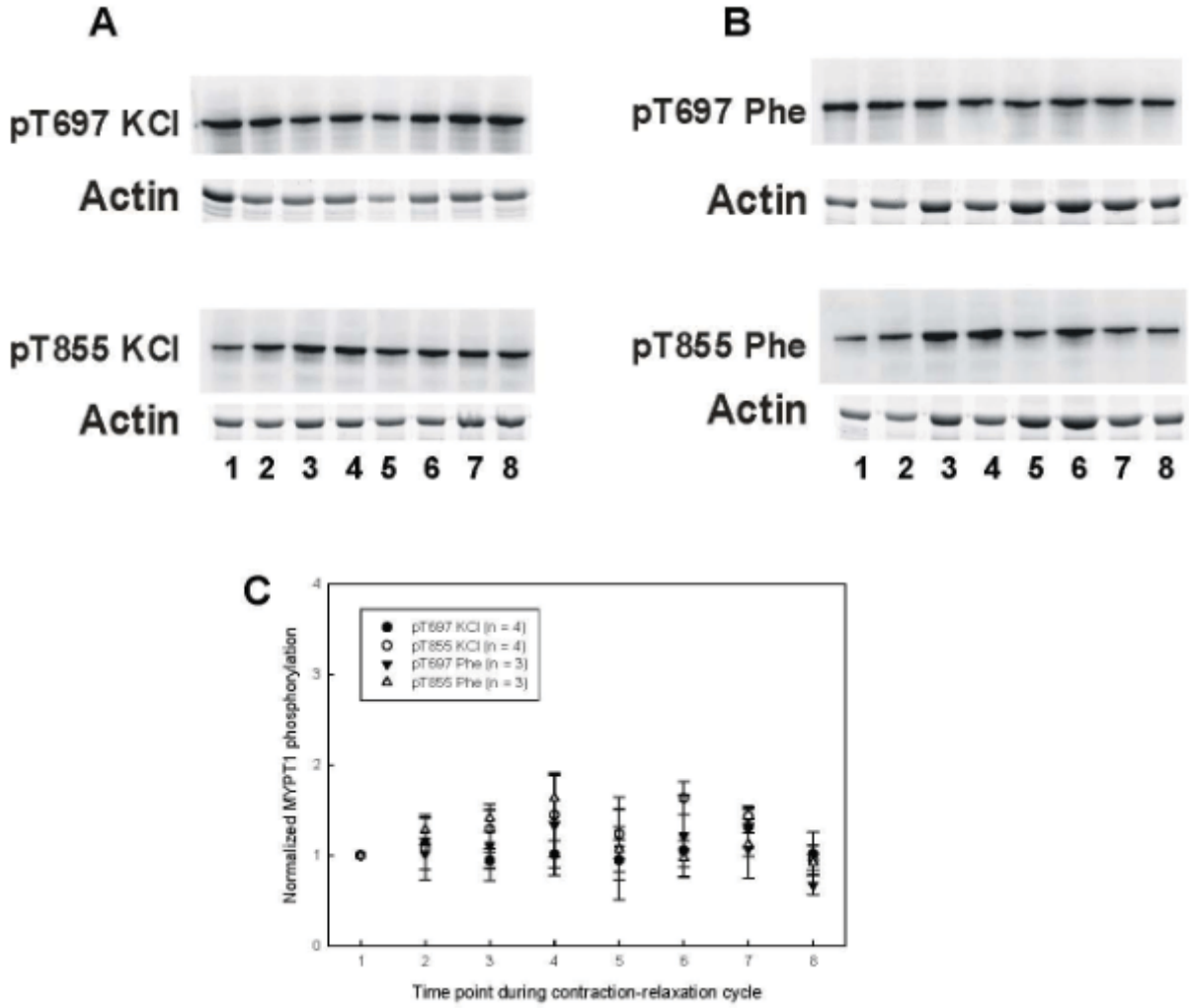
A
pT697 KCl
Actin
pT855 KCl
Actin
1 2 3 4 5 6 7 8
B
pT697 Phe
Actin
pT855 Phe
Actin
1 2 3 4 5 6 7 8
C
pT697 KCl (n = 4)
pT855 KCl (n = 4)
pT697 Phe (n = 3)
pT855 Phe (n = 3)
Normalized MYPT1 phosphorylation
0
1
2
3
4
1 2 3 4 5 6 7 8
Time point during contraction-relaxation cycle

FIGURE 7

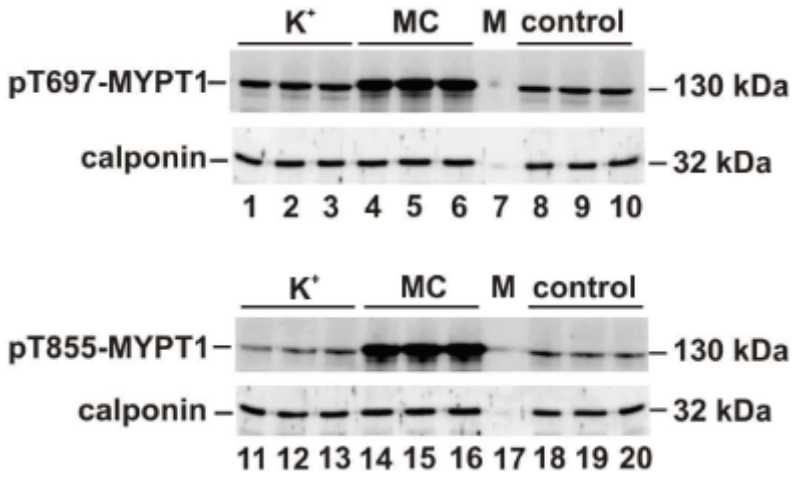
K+
MC
M
control
pT697-MYPT1
130 kDa
calponin
32 kDa
1 2 3 4 5 6 7 8 9 10
K+
MC
M
control
pT855-MYPT1
130 kDa
calponin
32 kDa
11 12 13 14 15 16 17 18 19 20

FIGURE 8

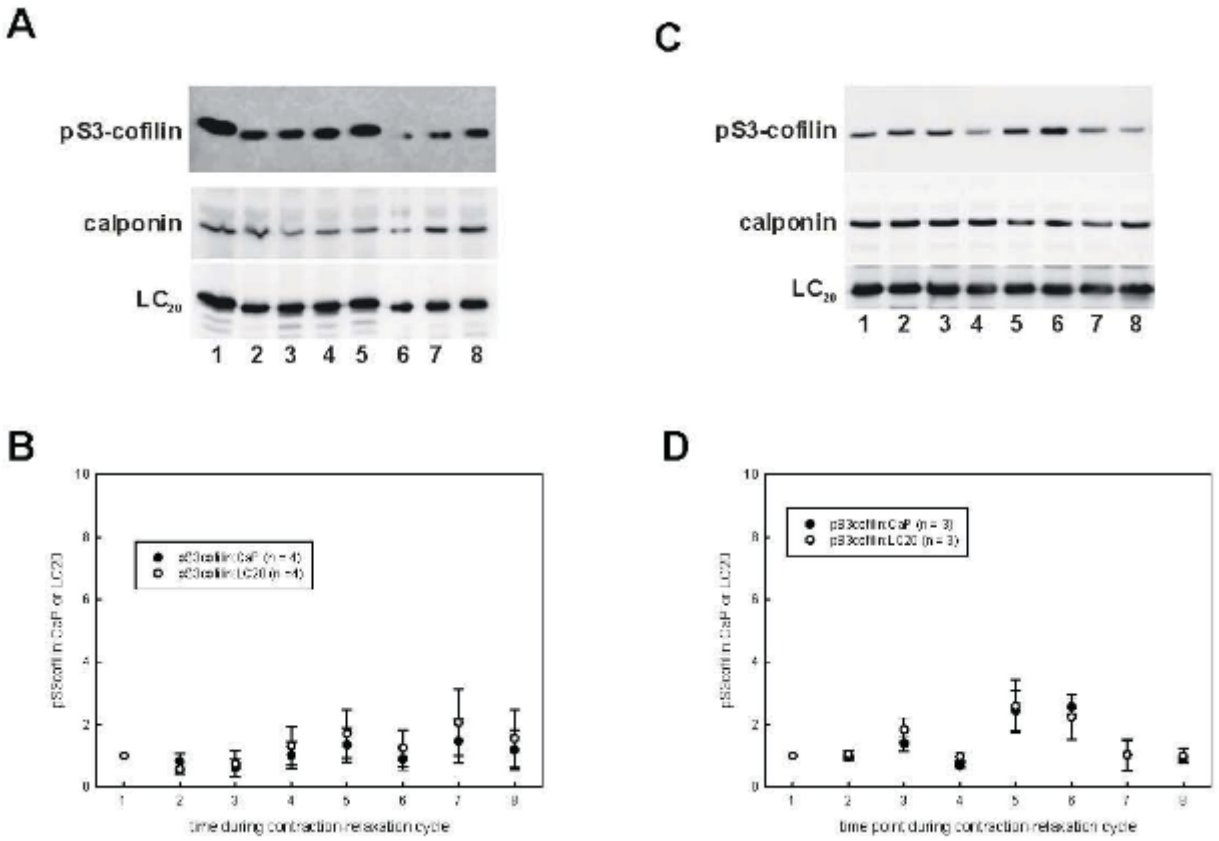
A
pS3-cofilin
calponin
LC20
1 2 3 4 5 6 7 8
C
pS3-cofilin
calponin
LC20
1 2 3 4 5 6 7 8
B
time during contraction relaxation cycle
D
time point during contraction relaxation cycle

FIGURE 9

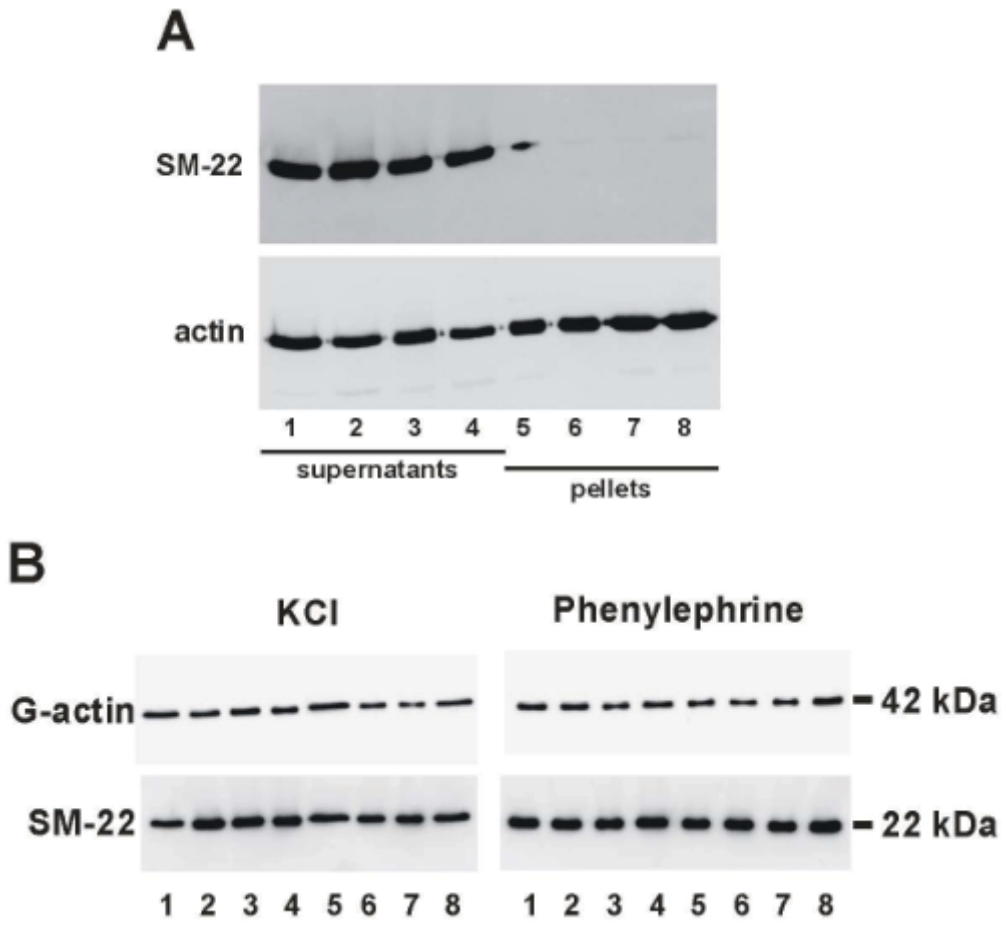
A
SM-22
actin
1 2 3 4 5 6 7 8
supernatants
pellets
B
KCl
Phenylephrine
G-actin
SM-22
42 kDa
22 kDa
1 2 3 4 5 6 7 8
1 2 3 4 5 6 7 8